Published by Institute of Physics Publishing for SISSA

Received: *May 27, 2008*
Accepted: *July 9, 2008*
Published: *July 24, 2008*

CP asymmetries in $\bar{B} \to \bar{K}^*(\to \bar{K}\pi)\bar{l}l$ and untagged $\bar{B}_s, B_s \to \phi(\to K^+K^-)\bar{l}l$ decays at NLO

Christoph Bobeth, Gudrun Hiller and Giorgi Piranishvili

Institut für Physik, Technische Universität Dortmund,
D-44221 Dortmund, Germany
E-mail: christoph.bobeth@uni-dortmund.de, ghiller@physik.uni-dortmund.de, giorgi.piranishvili@uni-dortmund.de

Abstract: The decay $\bar{B} \to \bar{K}^*(\to \bar{K}\pi)\bar{l}l$ offers great opportunities to explore the physics at and above the electroweak scale by means of an angular analysis. We investigate the physics potential of the seven CP asymmetries plus the asymmetry in the rate, working at low dilepton mass using QCD factorization at next-to leading order (NLO). The $b \to s$ CP asymmetries are doubly Cabibbo-suppressed $\lesssim 1\%$ in the Standard Model and its extensions where the CKM matrix is the only source of CP violation. Three CP asymmetries are T-odd, and can be $\mathcal{O}(1)$ in the presence of non-standard CP violation. The T-even asymmetries can reach $\mathcal{O}(0.1)$, limited by the small strong phases in the large recoil region. We furthermore point out an easy way to measure CP phases from time-integrated, untagged $\bar{B}_d, B_d \to K^*(\to K^0\pi^0)\bar{l}l$ and $\bar{B}_s, B_s \to \phi(\to K^+K^-)\bar{l}l$ decays. Analyses of these CP asymmetries can rule out, or further support the minimal description of CP violation through the CKM mechanism. Experimental studies are promising for (super) flavor factories and at hadron colliders.

Keywords: Rare Decays, Beyond Standard Model, B-Physics, CP violation.

JHEP07(2008)106

Contents

JHEP07(2008)106

1. Introduction

The quest for physics beyond the Standard Model (SM) is of highest priority at current and future flavor facilities [1]. A promising direction is to look for CP symmetry breaking effects that cannot be accounted for with the SM's very predictive CKM-mechanism of CP and flavor violation for the quarks. Rare $b \to s$ transitions are such sensitive probes, since all CP violating effects in the SM receive a universal suppression of order 10^{-2} from the CKM matrix elements. Ongoing experimental efforts include those with hadronic decays such as $\bar{B}_s, B_s \to J/\Psi\phi$ at the Tevatron [2] and $b \to s\bar{s}s$ induced penguin modes, see, e.g., [3] for recent data.

We focus here on exclusive semileptonic decays induced by $b \to s\bar{l}l$, $l = e, \mu$, to explore the borders of the SM. The decays $\bar{B} \to \bar{K}\bar{l}l$ and $\bar{B} \to \bar{K}^*\bar{l}l$ have already been observed,

with their rate being in agreement with the SM. Investigations of more involved observables such as dilepton mass spectra, lepton angle distributions and dimuon to dielectron ratios are currently being pursued [4 – 6]. The decay $\bar{B} \to \bar{K}^* \bar{l} l$ with subsequent $\bar{K}^* \to \bar{K}\pi$ allows to extract further physics information through an angular analysis of the $\bar{K}\pi\bar{l}l$ final state [7], especially on the chirality content [8 – 10].

Here we study the eight CP asymmetries in $\bar{B} \to \bar{K}^*(\to \bar{K}\pi)\bar{l}l$ decays, the one in the decay rate plus seven more requiring angular information. We calculate the matrix elements to next-to-leading order (NLO) in the strong coupling and to lowest order (LO) in the $1/E$ expansion [11], where E denotes the energy of the emitted $\bar{K}^*$ in $\bar{B}$ rest frame. We work within QCD factorization (QCDF), which has been applied to $\bar{B} \to \bar{K}^* \bar{l} l$ decays [12, 13], for analyses in soft-collinear effective theory (SCET), see [14]. Previous works on CP asymmetries in the angular distributions [7, 15, 16] employed naive factorization, see [17] for a PQCD study.

By means of the large energy limit, the QCDF framework used in our analysis holds for small dilepton invariant masses, and predicts small strong phases: Lowest order quark loops are either close to or below threshold, hence real (charm quarks), or CKM suppressed or induced by small penguin contributions (the lighter quarks). Other sources of strong phases are from subleading spectator effects or higher order in α_s.

This highlights T-odd CP asymmetries, three of which are accessible with the angular analysis. (The T-transformation reverses the sign of all particle momenta and spins.) The important feature is that the T-odd asymmetries are $\propto \cos\Delta_S \sin\Delta_W$, where Δ_S and Δ_W denote the differences of strong and weak phases, respectively. While the T-even CP asymmetries $\propto \sin\Delta_S \sin\Delta_W$ vanish for small strong phases, the T-odd asymmetries exhibit maximal sensitivity to CP violation in this limit.

Time-dependent CP asymmetries in $\bar{B}_d, B_d \to K^*(\to K^0\pi^0)\bar{l}l$ have also been considered in [16]. These measurements require large amounts of data. We suggest here to use the CP-odd property of four of the asymmetries to extract them from an untagged and time-integrated data set. It has been known that such data sets are useful to access CP violation in angular distributions, e.g., [18, 19]. We work out the corresponding CP-sensitive observables in $\bar{B}_d, B_d \to K^*(\to K^0\pi^0)\bar{l}l$ and $\bar{B}_s, B_s \to \phi(\to K^+K^-)\bar{l}l$ decays. The $K^+K^-\bar{l}l$ final state is the same as the one of the $\bar{B}_s, B_s \to \phi(\to K^+K^-)J/\Psi(\to \bar{l}l)$ decays, which are already under experimental study including angular analysis [2].

In section 2 we review the $\bar{B} \to \bar{K}^*(\to \bar{K}\pi)\bar{l}l$ angular distributions. CP asymmetries and possibilities of their measurement from double- and single-differential distributions are given in section 3. Prospects for $\bar{B}_d, B_d \to K^*(\to K^0\pi^0)\bar{l}l$ and $\bar{B}_s, B_s \to \phi(\to K^+K^-)\bar{l}l$ decays without tagging are examined in section 4. SM predictions and theoretical uncertainties are presented in section 5. In section 6 we model-independently investigate the impact of New Physics (NP) on the CP asymmetries. To do so, we work out constraints from other rare decay data, $\bar{B} \to X_s\bar{l}l, X_s\gamma$, the forward-backward asymmetry in $\bar{B} \to \bar{K}^*\bar{l}l$ and time-dependent CP asymmetries in $\bar{B}_d, B_d \to K^*(\to K^0\pi^0)\gamma$. We summarize in section 7. Various appendices A–F contain details of the calculation of the CP asymmetries.

JHEP07(2008)106

2. Full angular distribution

In this section we review the angular distribution of the exclusive decay $\bar{B} \to \bar{K}^*(\to \bar{K}\pi)\bar{l}l$ and its conjugate decay. Throughout this work we use $\bar{B} \equiv (b\bar{q})$ for $q = u, d$, $\bar{B}_s \equiv (b\bar{s})$ and $\bar{K}, \bar{K}^* \equiv (s\bar{q})$. We illustrate the kinematics for neutral mesons decaying to charged particles. Charged B-decays can be treated analogously. We discuss meson mixing effects and $\bar{B}_s \to \phi(\to K^+K^-)\bar{l}l$ decays in section 4.

The full angular distribution of the decay $\bar{B}^0 \to \bar{K}^{*0}(\to K^-\pi^+)\bar{l}l$ can be written in the limit of an on-shell decaying K^* resonance as a 4-differential distribution [7, 9]

$$\frac{d^4\Gamma}{dq^2\, d\cos\theta_l\, d\cos\theta_{K^*}\, d\phi} = \frac{3}{8\pi} J(q^2, \theta_l, \theta_{K^*}, \phi), \tag{2.1}$$

where the lepton spins have been summed over. Here, q^2 is the dilepton invariant mass squared, that is, q^μ is the sum of $p^\mu_{l^+}$ and $p^\mu_{l^-}$, the four momenta of the positively and negatively charged lepton, respectively. Furthermore, θ_l is defined as the angle between the negatively charged lepton and the $\bar{B}$ in the dilepton center of mass system (c.m.s.) and θ_{K^*} is the angle between the Kaon and the $\bar{B}$ in the $(K^-\pi^+)$ c.m.s... We denote by $\mathbf{p}_i$ the three momentum vector of particle i in the $\bar{B}$ rest frame. Then, ϕ is given by the angle between $\mathbf{p}_{K^-} \times \mathbf{p}_{\pi^+}$ and $\mathbf{p}_{l^-} \times \mathbf{p}_{l^+}$, i.e., the angle between the normals of the $(K^-\pi^+)$ and (l^-l^+) planes. The full kinematically accessible phase space is bounded by

$$4m_l^2 \leqslant q^2 \leqslant (M_B - M_{K^*})^2, \quad -1 \leqslant \cos\theta_l \leqslant 1, \quad -1 \leqslant \cos\theta_{K^*} \leqslant 1, \quad 0 \leqslant \phi \leqslant 2\pi, \tag{2.2}$$

where m_l, M_B and M_{K^*} denote the mass of the lepton, B meson and the K^*, respectively. For an off-resonance $\bar{B} \to \bar{K}\pi\bar{l}l$ study, see [20].

The dependence of the decay distribution (2.1) on the angles θ_l, θ_{K^*} and ϕ can be made explicit as

$$\begin{aligned} J(q^2, \theta_l, \theta_{K^*}, \phi) =& J_1^s \sin^2\theta_{K^*} + J_1^c \cos^2\theta_{K^*} + (J_2^s \sin^2\theta_{K^*} + J_2^c \cos^2\theta_{K^*})\cos 2\theta_l \\ &+ J_3 \sin^2\theta_{K^*} \sin^2\theta_l \cos 2\phi + J_4 \sin 2\theta_{K^*} \sin 2\theta_l \cos\phi + J_5 \sin 2\theta_{K^*} \sin\theta_l \cos\phi \\ &+ J_6 \sin^2\theta_{K^*} \cos\theta_l + J_7 \sin 2\theta_{K^*} \sin\theta_l \sin\phi \\ &+ J_8 \sin 2\theta_{K^*} \sin 2\theta_l \sin\phi + J_9 \sin^2\theta_{K^*} \sin^2\theta_l \sin 2\phi, \end{aligned} \tag{2.3}$$

where the coefficients $J_i^{(a)} = J_i^{(a)}(q^2)$ for $i = 1, \ldots, 9$ and $a = s, c$ are functions of the dilepton mass. In the following we suppress the q^2-dependence for brevity also in expressions derived from the $J_i^{(a)}$.

The angular coefficients $J_i^{(a)}$ can be expressed through the K^* transversity amplitudes $A_i(q^2)$ with $i = \{\perp, \parallel, 0, t\}$, see appendix A. Note that not all the $J_i^{(a)}$ are independent, for example, for vanishing lepton masses

$$3J_1^s = J_2^s, \qquad J_1^c = -J_2^c. \tag{2.4}$$

Furthermore, in the absence of right-handed currents $J_3 = J_9 = 0$ up to power corrections.

The corresponding distribution of the CP conjugated decay $B^0 \to K^{*0}(\to K^+\pi^-)\bar{l}l$ can be written as

$$\frac{d^4\bar{\Gamma}}{dq^2\, d\cos\theta_l\, d\cos\theta_{K^*}\, d\phi} = \frac{3}{8\pi}\bar{J}(q^2, \theta_l, \theta_{K^*}, \phi). \tag{2.5}$$

Here, θ_{K^*} denotes the angle between the Kaon and the B meson in the $(K^+\pi^-)$ c.m.s.. . . The definiton of θ_l is identical for both B and $\bar{B}$ decays. The angle ϕ for B decays is given by the angle between $\mathbf{p}_{K^+} \times \mathbf{p}_{\pi^-}$ and $\mathbf{p}_{l^-} \times \mathbf{p}_{l^+}$. Therefore, in the limit of unbroken CP, the distributions for B and $\bar{B}$ mesons are equal under the combined transformations $\theta_l \to \theta_l - \pi$ and $\phi \to -\phi$. The function $\bar{J}$ is hence obtained from J in (2.3) by the replacements

$$J^{(a)}_{1,2,3,4,7} \to \bar{J}^{(a)}_{1,2,3,4,7}, \qquad\qquad J_{5,6,8,9} \to -\bar{J}_{5,6,8,9}, \tag{2.6}$$

where $\bar{J}^{(a)}_i$ equals $J^{(a)}_i$ with all weak phases being conjugated [7].

With its rich multi-dimensional structure, the angular distributions in (2.1) and (2.5) have sensitivity to various effects modifying the SM, such as CP violation beyond CKM and/or right-handed currents. Given sufficient data, all $J^{(a)}_i$ and $\bar{J}^{(a)}_i$ can in principle be completely measured from the full angular distribution in all three angles θ_l, θ_{K^*} and ϕ.

The familiar dilepton invariant mass spectrum for $\bar{B} \to \bar{K}^*\bar{l}l$ decays can be recovered after integration over all angles as

$$\frac{d\Gamma}{dq^2} = J_1 - \frac{J_2}{3}, \quad \text{where} \;\; J_{1,2} \equiv 2J^s_{1,2} + J^c_{1,2}. \tag{2.7}$$

The (normalized) forward-backward asymmetry $A_{\rm FB}$ is given after full ϕ and θ_{K^*} integration as[1]

$$A_{\rm FB}(q^2) \equiv \left[\int_0^1 - \int_{-1}^0\right] d\cos\theta_l \, \frac{d^2\Gamma}{dq^2\, d\cos\theta_l} \Bigg/ \frac{d\Gamma}{dq^2} = J_6 \Bigg/ \frac{d\Gamma}{dq^2}. \tag{2.8}$$

By $d\bar{\Gamma}/dq^2$ and $\bar{A}_{\rm FB}(q^2)$ we refer to the corresponding spectra of the CP conjugated decays.

3. CP asymmetries

CP violating effects in the angular distribution are signaled by non-vanishing differences between the (q^2-dependent) angular coefficients

$$\Delta J^{(a)}_i = \Delta J^{(a)}_i(q^2) \equiv J^{(a)}_i - \bar{J}^{(a)}_i. \tag{3.1}$$

Of particular importance are the asymmetries related to the coefficients $J_{7,8,9}$. These are odd under $\phi \to -\phi$, and hence induce T-odd asymmetries $\Delta J_{7,8,9}$ which are not suppressed by small strong phases as predicted from QCDF.

The CP asymmetry in the dilepton mass distribution is commonly defined as, see (2.7),

$$A_{\rm CP}(q^2) \equiv \frac{d(\Gamma - \bar{\Gamma})}{dq^2} \Bigg/ \frac{d(\Gamma + \bar{\Gamma})}{dq^2} = \frac{1}{N_\Gamma}\left[\Delta J_1 - \frac{\Delta J_2}{3}\right], \quad N_\Gamma = N_\Gamma(q^2) = \frac{d(\Gamma + \bar{\Gamma})}{dq^2}. \tag{3.2}$$

[1]Since we define the lepton angle θ_l with respect to the l^-, our definiton of the forward-backward asymmetry (2.8) differs from the one in other works using the l^+, e.g., [5, 6, 12, 13, 21], by a global sign.

Following [7], we define in addition to $A_{\rm CP}$ seven normalized CP asymmetries as

$$A_i(q^2) \equiv \frac{2\Delta J_i}{N_\Gamma} \quad \text{for } i = 3,6,9, \qquad A_i^D(q^2) \equiv -\frac{2\Delta J_i}{N_\Gamma} \quad \text{for } i = 4,5,7,8. \tag{3.3}$$

Note that up to differences in the normalization A_6 equals the forward-backward CP asymmetry $A_{\rm FB}^{\rm CP}$ advocated to search for non-standard CP violation in the decay $\bar{B} \to \bar{K}^* \bar{l} l$ [22, 23], see (2.8). For q^2-integrated quantities we introduce the notation

$$\langle X \rangle = \int_{q^2_{\rm min}}^{q^2_{\rm max}} dq^2\, X(q^2), \tag{3.4}$$

where the integration from $q^2_{\rm min}$ to $q^2_{\rm max}$ should be in the low dilepton mass region in order to use the $1/E$ expansion of QCD for theory predictions, see appendix C. We then define the normalized q^2-integrated CP asymmetries as

$$\langle A_i \rangle \equiv 2\frac{\langle \Delta J_i \rangle}{\langle N_\Gamma \rangle} \quad \text{for } i = 3,6,9, \qquad \left\langle A_i^D \right\rangle \equiv -2\frac{\langle \Delta J_i \rangle}{\langle N_\Gamma \rangle} \quad \text{for } i = 4,5,7,8, \tag{3.5}$$

where the numerator and the denominator are integrated with the same q^2 cuts.

The CP asymmetries $\langle A_i \rangle$ $(i = 3,6,9)$ can, for example, be extracted from the double-differential distribution in θ_l and ϕ,

$$\begin{aligned}\frac{d^2\langle \Gamma \rangle}{d\cos\theta_l\, d\phi} = \frac{1}{4\pi}\big\{ &\langle J_1 \rangle + \langle J_2 \rangle \cos 2\theta_l + 2\langle J_3 \rangle \sin^2\theta_l \cos 2\phi \\ &+ 2\langle J_6 \rangle \cos\theta_l + 2\langle J_9 \rangle \sin^2\theta_l \sin 2\phi \big\},\end{aligned} \tag{3.6}$$

which is obtained from integrating (2.1) over θ_{K^*}. After full θ_l-integration follows

$$\frac{d\langle \Gamma \rangle}{d\phi} = \frac{1}{2\pi}\left\{ \langle J_1 \rangle - \frac{\langle J_2 \rangle}{3} + \frac{4}{3}\langle J_3 \rangle \cos 2\phi + \frac{4}{3}\langle J_9 \rangle \sin 2\phi \right\}, \tag{3.7}$$

showing that $\langle \Delta J_9 \rangle$ can be found from $d\left\langle \Gamma + \bar{\Gamma} \right\rangle / d\phi$, whereas $\langle \Delta J_3 \rangle$ can be obtained from $d\left\langle \Gamma - \bar{\Gamma} \right\rangle / d\phi$, with $\langle \Delta J_1 \rangle - \langle \Delta J_2 \rangle /3$ from $A_{\rm CP}$ without angular study, see (3.2).

The measurement of the CP asymmetries $\langle A_i^D \rangle$ $(i = 4,5,7,8)$ requires binning into $\cos\theta_{K^*}$ as

$$\begin{aligned}\frac{d^2\left\langle A_{\theta_{K^*}} \right\rangle}{d\cos\theta_l\, d\phi} &\equiv \left[\int_0^1 - \int_{-1}^0\right] d\cos\theta_{K^*}\, \frac{d^3\langle \Gamma \rangle}{d\cos\theta_{K^*}\, d\cos\theta_l\, d\phi} \\ &= \frac{1}{2\pi}\big\{ \langle J_4 \rangle \sin 2\theta_l \cos\phi + \langle J_5 \rangle \sin\theta_l \cos\phi + \langle J_7 \rangle \sin\theta_l \sin\phi + \langle J_8 \rangle \sin 2\theta_l \sin\phi \big\}.\end{aligned} \tag{3.8}$$

From here follows upon full θ_l-integration

$$\frac{d\left\langle A_{\theta_{K^*}} \right\rangle}{d\phi} = \frac{1}{4}\left\{ \langle J_5 \rangle \cos\phi + \langle J_7 \rangle \sin\phi \right\}. \tag{3.9}$$

We learn that $\langle \Delta J_5 \rangle$ can be extracted from $d\left\langle A_{\theta_{K^*}} + \bar{A}_{\theta_{K^*}} \right\rangle / d\phi$ whereas $\langle \Delta J_7 \rangle$ can be obtained from $d\left\langle A_{\theta_{K^*}} - \bar{A}_{\theta_{K^*}} \right\rangle / d\phi$. The double asymmetry in θ_{K^*} and θ_l,

$$\frac{d\left\langle A_{\theta_{K^*},\theta_l} \right\rangle}{d\phi} \equiv \left[\int_0^1 - \int_{-1}^0\right] d\cos\theta_l\, \frac{d^2\left\langle A_{\theta_{K^*}} \right\rangle}{d\cos\theta_l\, d\phi} = \frac{2}{3\pi}\left\{ \langle J_4 \rangle \cos\phi + \langle J_8 \rangle \sin\phi \right\}, \tag{3.10}$$

JHEP07(2008)106

allows to obtain $\langle \Delta J_4 \rangle$ from $d\left\langle A_{\theta_{K^*},\theta_l} - \bar{A}_{\theta_{K^*},\theta_l} \right\rangle / d\phi$, whereas $\langle \Delta J_8 \rangle$ can be extracted from $d\left\langle A_{\theta_{K^*},\theta_l} + \bar{A}_{\theta_{K^*},\theta_l} \right\rangle / d\phi$.

The latter considerations demonstrate how the CP violating angular coefficients ΔJ_i for $i = 3, 4, 5, 7, 8, 9$ can be extracted from distributions in the angle ϕ. The quantity ΔJ_6 can be measured easiest from the $\cos\theta_l$-distribution, i.e., by adding the (numerators of the) forward-backward asymmetries $A_{\rm FB}$ and $\bar{A}_{\rm FB}$, see (2.8). Note that only A_3, A_6 and A_9 can be obtained from a genuinely single-differential distribution. A_9 is the only T-odd asymmetry with this property.

Analytical expressions for all CP asymmetries at NLO in terms of the short distance coefficients from the electroweak Hamiltonian in appendix B are presented in appendix D. In particular, we include NLO α_s-corrections thus present in this work the first analyses of CP asymmetries in the $\bar{B} \to \bar{K}^*(\to \bar{K}\pi)\bar{l}l$ angular distributions at this order.

Corrections from $B_d - \bar{B}_d$ mixing to the time integrated CP asymmetries in flavor specific (self-tagging) final states are of the order $|A^d_{\rm SL}| \lesssim \mathcal{O}(10^{-3})$ [24] and can be neglected. Here, $A^d_{\rm SL}$ denotes the semileptonic asymmetry into wrong sign leptons in the B_d-system.

4. CP asymmetries without tagging

With the J_i, $i = 5, 6, 8, 9$ being odd under CP, see (2.6), the corresponding CP asymmetries can be extracted from $d\Gamma + d\bar{\Gamma}$, i.e., without identifying the flavor of the initial b quark. This feature is very useful for $\bar{B}_d, B_d \to K^*(\to K^0\pi^0)\bar{l}l$ and $\bar{B}_s, B_s \to \phi(\to K^+K^-)\bar{l}l$ decays, which unlike $\bar{B}_d, B_d \to K^*(\to K^\mp\pi^\pm)\bar{l}l$ or charged B-decays, are not self-tagging. We focus here on B_s-decays to CP eigenstates, but the formalism equally applies to B_d-decays after the corresponding replacements.

Both $\bar{B}_s$ and B_s angular distributions are described by the angles θ_l, θ_{K^*} and ϕ. These are defined in complete analogy with $\bar{B} \to \bar{K}^*(\to \bar{K}\pi)\bar{l}l$ decays, see section 2: θ_l is the angle between the negatively charged lepton and the $\bar{B}_s/B_s$ in the dilepton c.m.s., θ_{K^*} denotes the angle between the K^- and the $\bar{B}_s/B_s$ in the (K^-K^+) c.m.s. and ϕ is the angle between $\mathbf{p}_{K^-} \times \mathbf{p}_{K^+}$ and $\mathbf{p}_{l^-} \times \mathbf{p}_{l^+}$.

To account for mixing, time-dependent transversity amplitudes need to be introduced:

$$A_a(t) \equiv A(\bar{B}_s(t) \to \phi(\to K^+K^-)_a\bar{l}l), \quad \bar{A}_a(t) \equiv A(B_s(t) \to \phi(\to K^+K^-)_a\bar{l}l), \quad (4.1)$$

where $A_a(t), (\bar{A}_a(t))$ denotes the amplitude for a meson born at time $t = 0$ as a $\bar{B}_s$, (B_s) decaying through the transversity amplitude $a = \perp, \|, 0$ at later times t. Here we use for brevity $A_a(t)$ for both $A^L_a(t)$ and $A^R_a(t)$. The formulae for the unmixed transversity amplitudes, i.e., the ones at $t = 0$ can be taken from appendix C with the requisite replacements in masses and hadronic parameters and differences in the spectator effects given in [13] to account for the $\bar{B}_s \to \phi$ transitions.

Untagged rates $d\Gamma + d\bar{\Gamma}$ can then be written as $(a, b = \perp, \|, 0)$ [18]

$$\begin{aligned}\bar{A}^*_b(t)\bar{A}_a(t) + A^*_b(t)A_a(t) = \frac{1}{2}A(B_s \to \phi(\to K^+K^-)_b\bar{l}l)^*A(B_s \to \phi(\to K^+K^-)_a\bar{l}l) \\ \times \left[(1 + \eta_a\eta_b\xi^*_b\xi_a)\left(e^{-\Gamma_L t} + e^{-\Gamma_H t}\right) + (\eta_b\xi^*_b + \eta_a\xi_a)\left(e^{-\Gamma_L t} - e^{-\Gamma_H t}\right)\right]. \quad (4.2)\end{aligned}$$

JHEP07(2008)106

Here, $\eta_{\parallel,0} = +1$ and $\eta_\perp = -1$ are the CP eigenvalues of the final state and $\Gamma_{L(H)}$ denotes the width of the lighter (heavier) mass eigenstate. We neglect CP violation in mixing, which is bounded by the semileptonic asymmetry in the B_s-system $|A^s_{\rm SL}| \lesssim \mathcal{O}(10^{-2})$ [2]. Furthermore,

$$\xi_a = e^{-i\Phi_M} \frac{A(\bar{B}_s \to \phi(\to K^+K^-)_a \bar{l}l)}{A(\bar{B}_s \to \phi(\to K^+K^-)_a \bar{l}l)(\delta_W \to -\delta_W)}, \tag{4.3}$$

where $(\delta_W \to -\delta_W)$ implies the conjugation of all weak phases in the denominator and Φ_M denotes the phase of the $B_s - \bar{B}_s$ mixing. It is very small in the SM, $\Phi_M^{\rm SM} = 2\arg(V_{ts}^* V_{tb})$.

The CP asymmetries $\Delta J_i(t) = J_i(t) - \bar{J}_i(t)$, $i = 5, 6, 8, 9$ are then obtained by taking the real and imaginary parts of (4.2), adding or subtracting $\bar{A}_b^{k*}(t)\bar{A}_a^k(t) + A_b^{k*}(t)A_a^k(t)$ for $k = L$ and $k = R$, and taking into account normalization factors depending on the angular coefficient J_i, see appendix A. After time-integration follows from (4.2)

$$\begin{aligned}\int_0^\infty dt(\bar{A}_b^*(t)\bar{A}_a(t) + A_b^*(t)A_a(t)) &= A(B_s \to \phi(\to K^+K^-)_b \bar{l}l)^* A(B_s \to \phi(\to K^+K^-)_a \bar{l}l) \\ &\times \frac{1}{\Gamma(1-y^2)} \left[(1 + \eta_a\eta_b\xi_b^*\xi_a) - y\,(\eta_b\xi_b^* + \eta_a\xi_a)\right], \quad y = \frac{\Delta\Gamma}{2\Gamma},\end{aligned} \tag{4.4}$$

where $\Gamma = (\Gamma_L + \Gamma_H)/2$ and the width difference $\Delta\Gamma = \Gamma_L - \Gamma_H$.

This expression (4.4) becomes transparent if one neglects strong phases, where $\xi_a = e^{-i(\Phi_M - 2\Phi_a)}$, $\Phi_a \equiv \arg(A(\bar{B}_s \to \phi(\to K^+K^-)_a \bar{l}l)$. For $a \neq b$, $\eta_a = -\eta_b$ we obtain

$$\begin{aligned}\int_0^\infty dt\,{\rm Im}(\bar{A}_b^*(t)\bar{A}_a(t) + A_b^*(t)A_a(t)) &= \frac{2}{\Gamma(1-y^2)} |A(B_s \to \phi(\to K^+K^-)_b \bar{l}l)| \\ &\times |A(B_s \to \phi(\to K^+K^-)_a \bar{l}l)| \cdot \left[\sin(\Phi_a - \Phi_b) - y\eta_a \sin(\Phi_M - \Phi_a - \Phi_b)\right],\end{aligned} \tag{4.5}$$

$$\begin{aligned}\int_0^\infty dt \sum_a (|\bar{A}_a(t)|^2 + |A_a(t)|^2) &= \frac{2}{\Gamma(1-y^2)} \sum_a |A(B_s \to \phi(\to K^+K^-)_a \bar{l}l)|^2 \\ &\times \left[1 - y\eta_a \cos(\Phi_M - 2\Phi_a)\right],\end{aligned} \tag{4.6}$$

where (4.5) gives the asymmetries related to $J_{8,9}$ and (4.6) is needed for normalization, that is, gives (twice) the CP averaged decay rate. It also exhibits sensitivity to CP phases. The T-even asymmetries associated with $J_{5,6}$ vanish with no strong phases present.

We define (q^2-dependent) CP-odd CP asymmetries $A_i^{(D)mix}$ as ($a = \perp, \parallel, 0$, $k = L, R$)

$$\begin{aligned} A_i^{\rm mix}(q^2) &\equiv 2\frac{\int_0^\infty dt \Delta J_i(t)}{\int_0^\infty dt \sum_{a,k}(|\bar{A}_a^k(t)|^2 + |A_a^k(t)|^2)} \qquad \text{for} \qquad i = 6, 9, \\ A_i^{Dmix}(q^2) &\equiv -2\frac{\int_0^\infty dt \Delta J_i(t)}{\int_0^\infty dt \sum_{a,k}(|\bar{A}_a^k(t)|^2 + |A_a^k(t)|^2)} \qquad \text{for} \qquad i = 5, 8, \end{aligned} \tag{4.7}$$

which match the CP asymmetries of the flavor-specific, unmixed decays (3.3) for $y \to 0$.

For B_d-mesons, y is below 10^{-2} [24], and the untagged and time-integrated $K^0\pi^0$ final states yield the same information on CP violation as the ones with $K^\mp\pi^\pm$ discussed in section 3, or charged B-decays. (For early works with $y = 0$, see [19]). For B_s-mesons the width difference is larger, $y \sim \mathcal{O}(0.1)$ [24], and interference effects become observable with

JHEP07(2008)106

$\lambda = 0.2258^{+0.0016}_{-0.0017}$	(95% C.L.) [26]	$\mathcal{B}(\bar{B} \to X_c l \bar{\nu}_l) = (10.57 \pm 0.15)\%$	[24]
$\lvert V_{cb}\rvert = 0.0417 \pm 0.0013$	(95% C.L.) [26]	$\tau_{B^0} = (1.530 \pm 0.009)$ ps	[24]
$\bar{\rho} = [0.108,\, 0.243]$	(95% C.L.) [26]	$\tau_{B_s} = (1.425 \pm 0.041)$ ps	[24]
$\bar{\eta} = [0.288,\, 0.375]$	(95% C.L.) [26]	$f_{B_{u,d}} = (200 \pm 30)$ MeV	
$\alpha_s(m_Z) = 0.1176 \pm 0.0020$	[24]	$f_{B_s} = (240 \pm 30)$ MeV	[28]
$\alpha_e(m_b) = 1/133$		$\lambda_{B,+}(1.5\text{ GeV}) = (0.458 \pm 0.115)$ GeV	[13, 29]
$m_W = 80.403$ GeV	[24]	$f_\perp^{K^*}(1\text{ GeV}) = (185 \pm 10)$ MeV	[30]
$m_t^{\text{pole}} = (170.9 \pm 1.8)$ GeV	[27]	$f_\parallel^{K^*} = (217 \pm 5)$ MeV	[24]
$m_b = (4.6 \pm 0.1)$ GeV	[12]	$a_{1,K^*}^{\perp,\parallel}(1\text{ GeV}) = 0.1 \pm 0.07$	[25]
$m_c^{\text{pole}} = (1.4 \pm 0.2)$ GeV		$a_{2,K^*}^{\perp,\parallel}(1\text{ GeV}) = 0.1 \pm 0.1$	[25]

Table 1: The numerical input used in our analysis. We denote by m_b the PS mass at the factorization scale $\mu_f = 2$ GeV. We neglect the strange quark mass throughout this work unless otherwise stated. The numerical input for the form factors $\xi_{\perp,\parallel}$ is given in appendix E.

the mixing phase Φ_M. The latter is currently under intense experimental study and only poorly determined to date, see, e.g., [2].

We refrain in this work from presenting a dedicated numerical analysis for the $\bar{B}_s, B_s \to \phi(\to K^+K^-)\bar{l}l$ observables $A_i^{(D)mix}$: The presumably dominant part independent of the width difference can be inferred from $\bar{B} \to \bar{K}^*(\to \bar{K}\pi)\bar{l}l$ decays by SU(3). The biggest corrections such as those from the form factors and phase space are expected to cancel in the asymmetries. On the other hand, discrepancies in the CP asymmetries between B_d- and B_s-processes at $\mathcal{O}(y)$ can be attributed to the mixing parameters y and Φ_M.

5. Standard model predictions

CP asymmetries in the decays of hadrons are in the SM solely induced by the CKM matrix. For the $b \to s$ transitions under consideration here, the requisite weak phase difference stems from $\hat{\lambda}_u = V_{ub}V_{us}^*/V_{tb}V_{ts}^*$. Therefore, all CP asymmetries in $\bar{B} \to \bar{K}^*(\to \bar{K}\pi)\bar{l}l$ decays discussed here receive an overall suppression by $\text{Im}[\hat{\lambda}_u] \simeq \bar{\eta}\lambda^2$ of order 10^{-2}, where λ and $\bar{\eta}$ denote parameters of the Wolfenstein parametrization of the CKM matrix.

We work out the SM CP asymmetries in $\bar{B} \to \bar{K}^*(\to \bar{K}\pi)\bar{l}l$ decays in the low-q^2 region using QCDF at NLO in α_s and leading order $1/E$. Analytical expressions for the asymmetries are given in appendix D. The CP asymmetries in the SM can be obtained by setting the NP Wilson coefficients $C_{7,9,10}^{(\prime),\text{NP}} = 0$, see appendix B for the effective Hamiltonian used. Details on the QCDF framework and the transversity amplitudes are given in appendix C. We take the $B \to K^*$ form factors from light cone QCD sum rules (LCSR) calculations [25], see appendix E. Our numerical input is compiled in table 1. We checked that our findings for the branching ratio and the forward-backward asymmetry of $\bar{B} \to \bar{K}^*\bar{l}l$ decays agree for the given input with [12, 13]. Our predictions always refer to neutral B-decays unless otherwise stated.

JHEP07(2008)106

The three main uncertainties in the asymmetries come from the form factors $\xi_\parallel$ and $\xi_\perp$, the variation of the renormalization scale μ_b and the CKM parameters. We vary the scale between $m_b/2$ and $2m_b$ and allow for an uncertainty of 11% and 14% for $\xi_\perp$ and $\xi_\parallel$, respectively. The CKM input is given in table 1. For the total uncertainty estimate, all three sources of uncertainty are added in quadrature.

In figure 1 we show the T-odd CP asymmetries $A_{7,8}^D$ and the T-even ones $A_{\rm CP}, A_{4,5}^D$ and A_6 as a function of q^2. The various bands indicate the uncertainties due to the form factors, the CKM parameters, μ_b and the total uncertainty. The asymmetries A_3 and A_9 are not shown, since they vanish in the SM at lowest order in $1/E$. (A small finite value is induced by the strange quark mass.) Hence, their leading contributions may arise as

$$A_{3,9} \sim \mathrm{Im}[\hat{\lambda}_u]\, \mathcal{O}(\Lambda/E) \sim \mathcal{O}(10^{-3}). \tag{5.1}$$

The LO predictions for the CP asymmetries are also included in figure 1. The higher order α_s-corrections increase the size of the CP asymmetries. For A_7^D and A_8^D this happens because their respective LO values are suppressed by cancellations. Specifically, in the SM

$$A_7^D \sim \mathrm{Im}[\hat{\lambda}_u]\mathrm{Re}\left[\frac{\mathcal{T}_\perp^{(u)}}{\xi_\perp} + \frac{q^2}{M_B^2}\frac{\mathcal{T}_\parallel^{(u)}}{\xi_\parallel}\right], \tag{5.2}$$

which vanishes at LO in QCDF, see (C.4), and also [15]. (Our value of A_7^D at LO is tiny but finite since in the numerical analysis we do not neglect kinematical factors $M_{K^*}^2/M_B^2$.) The asymmetry A_8^D is subject to similar cancellations, although here an additional LO term exists, which is, however, numerically subleading. The values of A_7^D and A_8^D are therefore determined by the NLO α_s-corrections resulting in a large μ_b uncertainty. The impact of the higher order terms on the T-even asymmetries is sizeable, but less pronounced. We discuss further details of the SM CP asymmetries in the context of the integrated CP asymmetries.

We find that all q^2-integrated CP asymmetries $\langle A_i^{(D)}\rangle$ are less than $\mathcal{O}\left(10^{-2}\right)$ in the SM. This can be seen in table 2, where we give the results for the two cuts $(q^2_{\rm min}, q^2_{\rm max}) = (1,6)$ GeV^2 (upper entries) and $(1,7)$ GeV^2 (lower entries), respectively. The uncertainties from the form factors and μ_b are also shown separately. Due to the overall CKM factor $\mathrm{Im}[\hat{\lambda}_u]$, all CP asymmetries suffer from a universal 15% uncertainty related to that. The corresponding values for the NLO CP averaged decay rates are $\langle N_\Gamma\rangle/2 = (1.1 \pm 0.3)\cdot 10^{-19}$ GeV and $\langle N_\Gamma\rangle/2 = (1.3^{+0.4}_{-0.3})\cdot 10^{-19}$ GeV for $(q^2_{\rm min}, q^2_{\rm max}) = (1,6)$ GeV^2 and $(1,7)$ GeV^2, respectively, assuming $\mathcal{B}(K^* \to K\pi) = 100\%$. The uncertainty in the rate is about 25 % from the form factors, 7 % from V_{ts} and order one percent from μ_b.

The form factor induced uncertainty in the asymmetries depends on the amount of cancellations between the numerator and the decay rate in the denominator. We recall that we vary the two form factors within their uncertainties independently. Taking into account correlations would reduce the errors in the ratios, but requires control over the parameters of the LCSR calculation [25], which is beyond the scope of this work. Since the decay rate is dominated by the longitudinal K^* polarization driven by $\xi_\parallel$, see the discussion following (C.7), the strongest form factor uncertainty is seen in A_6 being proportional to

JHEP07(2008)106

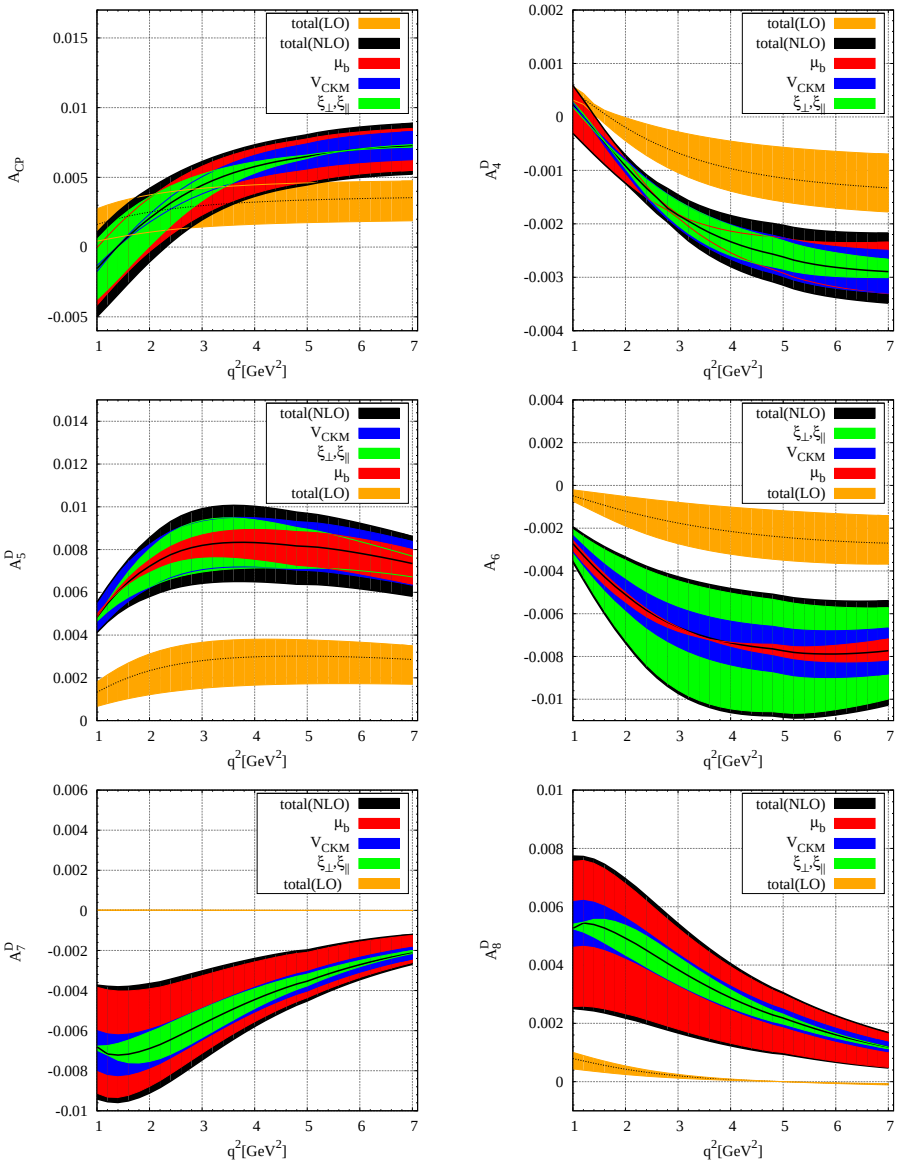

Figure 1: The CP asymmetries $A_{\mathrm{CP},6}(q^2)$ and $A^D_{4,5,7,8}(q^2)$ in the SM in the low-q^2 region at LO and NLO in QCDF. The various bands show the uncertainty due to the form factors, the CKM parameters and μ_b separately, whereas the overall band indicates the total uncertainty.

$\xi_\perp^2$. The other asymmetries A_i^D, $i = 4, 5, 7, 8$ with numerator $\propto \xi_\parallel \xi_\perp$ receive more efficient cancellations.

As can be seen from table 2, $\langle A_{\mathrm{CP}} \rangle$, $\langle A_7^D \rangle$ and $\langle A_8^D \rangle$ exhibit a massive μ_b dependence of order 50 %. The CP asymmetries $A_i^{(D)}$ with $i = 4, 5, 6$ are not subject to the cancellations mentioned after (5.2) and have a smaller residual μ_b uncertainty below ten percent. The μ_b dependence of $\langle A_6 \rangle$ of a few percent is accidentally small due to significant cancellations between different q^2-regions, see the crossing of the μ_b bands in A_6 near $q^2 \simeq (3-4)\,\mathrm{GeV}^2$ in figure 1.

JHEP07(2008)106

	SM $\cdot 10^{-3}$	$\xi_{\perp,\parallel}$[%]	μ_b[%]	SM LO $\cdot 10^{-3}$	SM($B^{\mp}$) $\cdot 10^{-3}$
$\langle A_{\rm CP}\rangle$	$4.2^{+1.7}_{-2.5}$	$^{+19}_{-24}$	$^{+33}_{-51}$	$3.0^{+1.2}_{-1.5}$	$10.0^{+2.3}_{-2.9}$
	$4.8^{+1.7}_{-2.4}$	$^{+13}_{-17}$	$^{+29}_{-44}$	$3.1^{+1.2}_{-1.6}$	$9.9^{+2.2}_{-2.8}$
$\langle A_4^D\rangle$	$-1.8^{+0.3}_{-0.3}$	$^{+11}_{-8}$	$^{+2}_{-6}$	$-0.7^{+0.4}_{-0.4}$	$-0.7^{+0.4}_{-0.3}$
	$-2.0^{+0.4}_{-0.4}$	$^{+11}_{-8}$	$^{+7}_{-8}$	$-0.8^{+0.5}_{-0.4}$	$-1.1^{+0.4}_{-0.4}$
$\langle A_5^D\rangle$	$7.6^{+1.5}_{-1.6}$	$^{+10}_{-13}$	$^{+7}_{-8}$	$2.7^{+0.8}_{-1.2}$	$10.0^{+2.2}_{-2.3}$
	$7.6^{+1.5}_{-1.6}$	$^{+9}_{-12}$	$^{+7}_{-9}$	$2.7^{+0.8}_{-1.2}$	$9.8^{+2.1}_{-2.1}$
$\langle A_6\rangle$	$-6.4^{+2.2}_{-2.7}$	$^{+31}_{-39}$	$^{+0}_{-2}$	$-1.9^{+1.0}_{-0.9}$	$-6.3^{+2.1}_{-2.6}$
	$-6.7^{+2.2}_{-2.7}$	$^{+30}_{-37}$	$^{+1}_{-3}$	$-2.0^{+1.1}_{-1.0}$	$-6.6^{+2.2}_{-2.7}$
$\langle A_7^D\rangle$	$-5.1^{+2.4}_{-1.6}$	$^{+11}_{-8}$	$^{+42}_{-26}$	$< 10^{-2}$	$-7.1^{+2.6}_{-1.9}$
	$-4.6^{+2.1}_{-1.4}$	$^{+10}_{-6}$	$^{+42}_{-25}$		$-6.5^{+2.3}_{-1.7}$
$\langle A_8^D\rangle$	$3.5^{+1.4}_{-2.0}$	$^{+7.4}_{-10}$	$^{+37}_{-53}$	$0.2^{+0.04}_{-0.08}$	$3.4^{+1.4}_{-2.0}$
	$3.1^{+1.3}_{-1.7}$	$^{+6}_{-10}$	$^{+37}_{-53}$	$0.14^{+0.03}_{-0.06}$	$3.1^{+1.3}_{-1.8}$
$\langle A_{3,9}\rangle^{\dagger}$	$\mathcal{O}(1)$			$\mathcal{O}(1)$	$\mathcal{O}(1)$

Table 2: SM predictions for the integrated CP asymmetries in units of 10^{-3} with the integration boundaries $(q^2_{\rm min}, q^2_{\rm max}) = (1,6), (1,7)$ GeV^2 (from top to bottom). We take into account uncertainties from the form factors, the scale dependence μ_b and the CKM parameters, all of them added in quadrature for the total uncertainty. The relative uncertainties due to $\xi_\perp, \xi_\parallel$ and μ_b are also shown separately. The asymmetries at LO in α_s and the NLO ones for charged B-decays are given as well, see text for details. †The leading contributions $\langle A_{3,9}\rangle$ in the SM are power counting estimates only.

Furthermore, we study the impact of higher order contributions in QCDF on the $\langle A_i^{(D)}\rangle$. The shift from LO in α_s to NLO is substantial. Switching off the spectator interactions reduces the size of $\langle A^D_{7,8}\rangle$ by about 10 %, and by less for the other asymmetries. We also give in table 2 the NLO SM predictions for charged B-decays. The splitting between the CP asymmetries in neutral versus charged B-decays is dominated by weak annihilation contributions from current-current operators and varies a lot in size: $\langle A^D_{5,7}\rangle$ ($\langle A_{\rm CP}\rangle$) increase by $\mathcal{O}(30\%)$ (a factor of two) from neutral to charged B-decays, whereas $\langle A_4^D\rangle$ decreases by $\sim 1/2$. The splitting for $\langle A^{(D)}_{6,8}\rangle$ is at the few percent level.

The SM predictions for the untagged, time-integrated CP asymmetries $\langle A_i^{(D)mix}\rangle$, $i = 5,6,8,9$, in $\bar{B}_s, B_s \to \phi(\to K^+K^-)\bar{l}l$ decays (4.7) can be inferred from the $\langle A_i^{(D)}\rangle$ in neutral B_d-decays, which are given in table 2. Corrections arise from SU(3) flavor breaking, which is expected to be small in the ratios, from the B_s-width difference at the level of ten percent and from spectator interactions. All these effects are subdominant with respect to the theoretical uncertainties of the SM predictions.

6. Beyond the standard model

This section contains the model-independent analysis of the CP asymmetries. We consider

JHEP07(2008)106

observable	SM	data
$\mathcal{B}(\bar{B} \to X_s\gamma)^a$	$(3.15 \pm 0.23) \cdot 10^{-4}$ [34]	$(3.52 \pm 0.25) \cdot 10^{-4}$ [3]
$S^b_{K^*\gamma}$	$(-2.8^{+0.4}_{-0.5}) \cdot 10^{-2}$	-0.19 ± 0.23 [3, 31]
$\mathcal{B}(\bar{B} \to X_s\bar{l}l)\vert_{[1,6]}$	$(1.59 \pm 0.11) \cdot 10^{-6}$ [35]	$(1.60 \pm 0.51) \cdot 10^{-6}$ [33]
$\mathcal{B}(\bar{B} \to X_s\bar{l}l)\vert_{[>0.04]}$	$(4.15 \pm 0.70) \cdot 10^{-6}$ [21]	$(4.5 \pm 1.0) \cdot 10^{-6}$ [24]
$\langle A_{\rm FB}\rangle^c_{[high\,q^2]}$	< 0	$-(0.76^{+0.52}_{-0.32} \pm 0.07)$ [6], also [4, 5]
$\mathcal{B}(\bar{B}_s \to \bar{\mu}\mu)$	$\simeq 3 \cdot 10^{-9}$	$< 4.7 \cdot 10^{-8}$ at 90% C.L. [32]

Table 3: Relevant $b \to s\gamma$ and $b \to s\bar{l}l$ observables. [a]With photon energy cut $E_\gamma > 1.6\,\text{GeV}$. [b]SM value obtained with $m_s = 0.12$ GeV. [c]Note the different lepton angle convention between [5, 6] and this work.

NP contributions to the operators $\mathcal{O}_{7,9,10}$ which are part of the effective Hamiltonian (B.1) of the SM, as well as NP contributions to the chirality flipped ones $\mathcal{O}'_{7,9,10}$. We allow the respective NP coefficients $C_i^{\rm NP}$ and $C_i'^{\rm NP} = C_i'$ for $i = 7, 9, 10$ to vary in magnitude and phase, denoted by ϕ_i, within the constraints from the FCNC B-decay data. The radiative and semileptonic $b \to s$ transitions are the most important ones for our analysis. The relevant data and SM predictions are given in table 3.

In our analysis the NP Wilson coefficients are leading order coefficients. All Wilson coefficients are understood as evaluated at the low, μ_b-scale. We start with a discussion of the experimental constraints.

6.1 Experimental constraints

The radiative decays induced by $b \to s\gamma$ probe the electromagnetic dipole coefficients C_7 and C_7'. In the NP scenarios considered here, the flipped dipole coefficient has no interference terms in the radiative decay rates. Hence, these observables constrain only the magnitude of C_7' and not its phase.

We take into account the $\bar{B} \to X_s\gamma$ branching ratio for which we adopt the NNLO SM results from [34]. To account for the missing higher order calculation of the beyond-the-SM amplitude, we take for the theoretical uncertainty of the NP contribution twice the SM uncertainty. We apply the experimental constraints at 90 % C.L. We checked that the direct CP asymmetry in $\bar{B} \to X_s\gamma$, e.g., [36], does not give constraints beyond those from the $\bar{B} \to X_s\gamma$ branching ratio.

The time-dependent CP asymmetry $S_{K^*\gamma}$ in $\bar{B}_d, B_d \to K^{*0}(\to K^0\pi^0)\gamma$ [37] is important since it is sensitive to the interference of photons with different polarization, that is, photons coming from $\mathcal{O}_7$ versus $\mathcal{O}'_7$. To illustrate the dependence on the Wilson coefficients, we give $S_{K^*\gamma}$ at lowest order (indicated by the superscript (0) for the contributions already present in the SM):

$$S_{K^*\gamma} = -\frac{2|r|}{1+|r|^2}\sin\left(2\beta - \arg(C_7^{(0)}C_7')\right), \qquad r = C_7'/C_7^{(0)}\,. \tag{6.1}$$

Here we assume that there is no beyond-the-SM physics in $B_d - \bar{B}_d$-mixing, and its phase is given by the CKM matrix elements. We calculate the exclusive $\bar{B} \to \bar{K}^*\gamma$ decay amplitude

JHEP07(2008)106

with QCD factorization following [13] including α_s-corrections. The constraints from $S_{K^*\gamma}$ exclude some regions with $|r|$ of order one, unless the CP phases conspire to suppress the sine in (6.1), see below.

The second class of constraints stems from the semileptonic transitions and applies to all Wilson coefficients we consider, $C_{7,9,10}^{(\prime)}$. The inclusive $\bar{B} \to X_s \bar{l}l$ decays can be predicted with high accuracy, in the low-q^2 region at the level of $\lesssim 10\%$ [35], but also the high-q^2 region is theoretically accessible. As can be seen in table 3, we utilize the integrated branching ratios in the low-q^2 region with $q^2 \in [1,6]\,\mathrm{GeV}^2$, $\mathcal{B}(\bar{B} \to X_s \bar{l}l)|_{[1,6]}$, as well as for $q^2 > 0.04\,\mathrm{GeV}^2$, $\mathcal{B}(\bar{B} \to X_s \bar{l}l)|_{[>0.04]}$. The latter has been experimentally obtained by cutting out events with q^2 close to the first and second charmonium resonance, hence bears some model-dependence. We use the corresponding theory predictions from [35] and [21], respectively. The decay distributions with NP are given in [38]. The treatment of uncertainties is as for the $\bar{B} \to X_s\gamma$ branching ratio.

Concerning the exclusive $\bar{B} \to \bar{K}\bar{l}l$ and $\bar{B} \to \bar{K}^*\bar{l}l$ decays, we do not use the branching ratios for our model-independent analysis: the constraints are in general weaker than the ones from $\mathcal{B}(\bar{B} \to X_s \bar{l}l)$ due to the larger theoretical and experimental uncertainties. A particular difficulty with the available exclusive semileptonic decay data is the presence of measurements with different dilepton mass cuts, some of which in addition include regions where QCDF or SCET does not apply.

We employ instead early data on the $\bar{B} \to \bar{K}^*\bar{l}l$ forward-backward asymmetry from Belle and BaBar [4–6]. While these measurements have large uncertainties, both experiments strongly support the sign of A_{FB} in the high-q^2 region above the second charmonium peak to be SM-like.

A rigorous theory calculation of the exclusive $\bar{B} \to \bar{K}^*\bar{l}l$ decays in this kinematical region can be facilitated with an operator product expansion in Λ/Q and m_c^2/Q^2 where $Q = \{\sqrt{q^2}, m_b\}$ put forward in [39]. The leading contribution and also the order m_c^2/Q^2 terms do not introduce new non-perturbative matrix elements beyond naive factorization. Corrections start to enter at $\mathcal{O}(\alpha_s\Lambda/Q)$. The framework holds at low recoil, $(M_B - M_{K^*})^2 - 2M_B\Lambda \lesssim q^2 < (M_B - M_{K^*})^2$, which covers the large dilepton mass region above the Ψ' resonance, $q^2 \gtrsim 14\,\mathrm{GeV}^2$.

To leading order in the $1/Q$-expansion we obtain A_{FB} at low recoil as

$$A_{\mathrm{FB}}(q^2) \propto \mathrm{Re}\left[\left(C_9^{\mathrm{eff}}(q^2) + \frac{2m_b^2}{q^2}C_7^{\mathrm{eff}}\right) C_{10}^* - \left(C_9' + \frac{2m_b^2}{q^2}C_7'\right) C_{10}'^*\right]. \tag{6.2}$$

The effective coefficients read as $C_9^{\mathrm{eff}}(q^2) = C_9 + (4/3\,C_1 + C_2)g(q^2) + \cdots$ and $C_7^{\mathrm{eff}} = C_7 + \cdots$, where $4/3\,C_1 + C_2 \simeq 0.61$ are the dominant SM coefficients. The full expressions including the higher order α_s-corrections and the QCD penguin contributions are given in [39] and are included in our numerical analysis. The lowest order charm loop function is given as

$$g(q^2) = \frac{8}{27} + \frac{4}{9}\left(\ln\frac{\mu^2}{q^2} + i\pi\right), \tag{6.3}$$

which agrees with the perturbative quark loop function for massless quarks. Interestingly, the dependence on form factors can be factored out in A_{FB} (6.2) at this order. We require then the sign of $\langle A_{\mathrm{FB}}\rangle$ integrated over $q^2 > 14\,\mathrm{GeV}^2$ to be negative.

JHEP07(2008)106

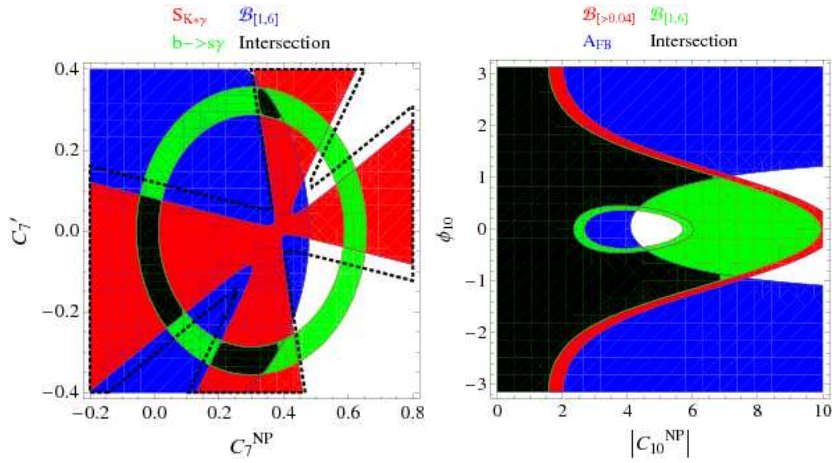

Figure 2: Allowed regions of Wilson coefficients in specific NP scenarios after applying the experimental constraints from radiative and semileptonic $b \to s$ processes as indicated. The black areas are allowed by all constraints. In the left panel we show C_7' versus $C_7^{\rm NP}$ assuming real Wilson coefficients. We give the magnitude of $C_{10}^{\rm NP}$ versus its CP phase ϕ_{10} in the right panel. In both plots all other NP Wilson coefficients have been set to zero. For details see text.

We show the impact of the FCNC constraints on the NP Wilson coefficients for two NP scenarios in figure 2. The areas allowed by all constraints are given in black. We learn that the observables (each shown in a different color) yield complementary information, and that the SM is allowed, as well as many significantly different NP solutions.

In the left plot, we entertain NP only in C_7 and C_7', and assume further no NP CP phases. The regions allowed by $\mathcal{B}(\bar{B} \to X_s\gamma)$, $S_{K^*\gamma}$ and $\mathcal{B}(\bar{B} \to X_s\bar{l}l)|_{[1,6]}$ are shown as the green ring, the red cross and the blue half circle, respectively. The impact of $S_{K^*\gamma}$ is significant. The semileptonic decay excludes in this NP scenario the flipped sign solution for the photonic dipole coefficient $C_7 \simeq -C_7^{\rm SM} \sim 0.31$. Note that dimensional analysis suggests that power corrections to r of the order $C_2\Lambda/(3m_bC_7) \sim 0.1$ may induce a larger SM contribution to $S_{K^*\gamma}$ than $\mathcal{O}(m_s/m_b)$ [40]. We show the resulting region in the $C_7'-C_7^{\rm NP}$-plane by the dashed lines in the left plot of figure 2. Because of the present experimental situation, however, the inclusion of the power corrections corresponds only to a small enlargement of the allowed parameter space. Note also that ref. [41] estimated the non-perturbative SM contributions to be smaller than the ones coming from naive power counting.

In the right plot we allow only for NP in C_{10}, and show the allowed regions in $|C_{10}^{\rm NP}|$ and the CP phase ϕ_{10}. Fixing the sign of $A_{\rm FB}$ (blue) and the semileptonic branching ratios $\mathcal{B}(\bar{B} \to X_s\bar{l}l)|_{[1,6]}$ (green) and $\mathcal{B}(\bar{B} \to X_s\bar{l}l)|_{[>0.04]}$ (red) yield orthogonal constraints. An upper bound on the magnitude of $C_{10}^{\rm NP}$ is obtained with the aid of $A_{\rm FB}$ as $|C_{10}^{\rm NP}| \lesssim 7$, improving on the bound from the branching ratios alone, $|C_{10}^{\rm NP}| \lesssim 10$.

6.2 CP asymmetries with new physics

The dependence of the CP asymmetries $A_i^{(D)}$ on the Wilson coefficients can be seen from the analytical (NLO) formulae in appendix D. We also provide numerical model-independent

JHEP07(2008)106

	generic NP	$C_{10}^{\rm NP}$ only	$C_{10}^{\prime\rm NP}$ only	$C_9^{\rm NP}$ only
$\langle A_{\rm CP}\rangle$	$[-0.12, 0.10]$	$[3, 8]\cdot 10^{-3}$	SM-like	$[-0.02, 0.02]$
$\langle A_3\rangle$	$[-0.08, 0.08]$	SM-like	SM-like	SM-like
$\langle A_4^D\rangle$	$[-0.04, 0.04]$	$[-4, -1]\cdot 10^{-3}$	$[-3, -1]\cdot 10^{-3}$	$[-0.01, 0.01]$
$\langle A_5^D\rangle$	$[-0.07, 0.07]$	$[-0.04, 0.04]$	$[-0.02, 0.04]$	$[5, 9]\cdot 10^{-3}$
$\langle A_6\rangle$	$[-0.13, 0.11]$	$[-0.05, 0.05]$	$[-9, -3]\cdot 10^{-3}$	SM-like
$\langle A_7^D\rangle$	$[-0.76, 0.76]$	$[-0.48, 0.48]$	$[-0.38, 0.38]$	SM-like
$\langle A_8^D\rangle$	$[-0.48, 0.48]$	$[2, 7]\cdot 10^{-3}$	$[-0.28, 0.28]$	$[-0.17, 0.17]$
$\langle A_9\rangle$	$[-0.62, 0.60]$	SM-like	$[-0.20, 0.20]$	SM-like
$\mathcal{B}(\bar{B}_s\to\bar{\mu}\mu)$	$< 1.4\cdot 10^{-8}$	$< 6.3\cdot 10^{-9}$	$< 1.3\cdot 10^{-8}$	SM

Table 4: The ranges of the integrated CP asymmetries $\langle A_i^{(D)}\rangle$ for $(q^2_{\rm min}, q^2_{\rm max}) = (1, 6)$ GeV^2 after applying the experimental constraints at 90% C.L. for the generic NP scenario and those with NP in C_{10}, C'_{10} or C_9 only. The upper limits on $\mathcal{B}(\bar{B}_s\to\bar{\mu}\mu)$ are also shown. For details see text.

formulae for the $\bar{B}\to\bar{K}^*(\to\bar{K}\pi)\bar{l}l$ branching ratio and CP asymmetries in appendix F. The numerators of $A^{(D)}_{\rm CP,3,4}$ are sensitive to $C_{7,9}$ and $C'_{7,9}$ whereas the numerators of $A^D_{5,7}$ and A_6 probe $C_{7,10}$ and $C'_{7,10}$. The numerators of $A^{(D)}_{8,9}$ can be affected by all Wilson coefficients considered here. Recall also that $A_{3,9}$ are very sensitive to the flipped Wilson coefficients since $A_{3,9}$ vanish in the limit $C'_i\to 0$ at lowest order in the $1/E$-expansion.

To see directly these features of the T-odd asymmetries, we provide LO formulae:

$$A_7^D = 2\mathcal{A}^D\frac{\hat{m}_b}{\hat{s}}(1-\hat{s})\mathrm{Im}\left[(C_{10}^{(0)}-C'_{10})(C_7^{\mathrm{eff}(0)}-C'_7)^*\right], \tag{6.4}$$

$$\begin{aligned} A_8^D = \mathcal{A}^D\beta_l\Big\{&\mathrm{Im}\Big[C_9^{(0)}C_9'^* + C_{10}^{(0)}C_{10}'^* + \frac{4\hat{m}_b^2}{\hat{s}}C_7^{\mathrm{eff}(0)}C_7'^* \\ &+\frac{\hat{m}_b}{\hat{s}}\big((1-\hat{s})(C'_7C_9'^* - C_7^{\mathrm{eff}(0)}C_9^{(0)*}) + (1+\hat{s})(C_7^{\mathrm{eff}(0)}C_9'^* - C'_7C_9^{(0)*})\big)\Big] \\ &-\mathrm{Re}(Y^{(0)})\mathrm{Im}\left[C'_9+\frac{\hat{m}_b}{\hat{s}}\big((1-\hat{s})C_7^{\mathrm{eff}(0)}+(1+\hat{s})C'_7\big)\right]\Big\} + \mathcal{O}(\hat{\lambda}_u), \end{aligned} \tag{6.5}$$

$$\begin{aligned} A_9 = 4\mathcal{A}^D\beta_l\Big\{&\mathrm{Im}\left[C_9^{(0)}C_9'^* + C_{10}^{(0)}C_{10}'^* + \frac{4\hat{m}_b^2}{\hat{s}^2}C_7^{\mathrm{eff}(0)}C_7'^* + \frac{2\hat{m}_b}{\hat{s}}(C_7^{\mathrm{eff}(0)}C_9'^* - C'_7C_9^{(0)*})\right] \\ &-\frac{\hat{m}_b}{\hat{s}}\mathrm{Re}(Y^{(0)})\mathrm{Im}\left[2C'_7+\frac{\hat{m}_b}{\hat{s}}C'_9\right]\Big\} + \mathcal{O}(\hat{\lambda}_u), \end{aligned} \tag{6.6}$$

where for A_8^D, A_9 we neglected SM CP violation suppressed by $\hat{\lambda}_u$, see appendix D for details.

We work out the CP asymmetries $\langle A_i^{(D)}\rangle$ with NP by taking into account the experimental constraints given in table 3. We consider scenarios with generic NP, that is, when all six NP Wilson coefficients are varied independently, and when varying only one coefficient at a time. The asymmetries are integrated over low dilepton masses, $q^2\in[1,6]$ GeV^2. Theoretical input parameters used are fixed at their central values.

JHEP07(2008)106

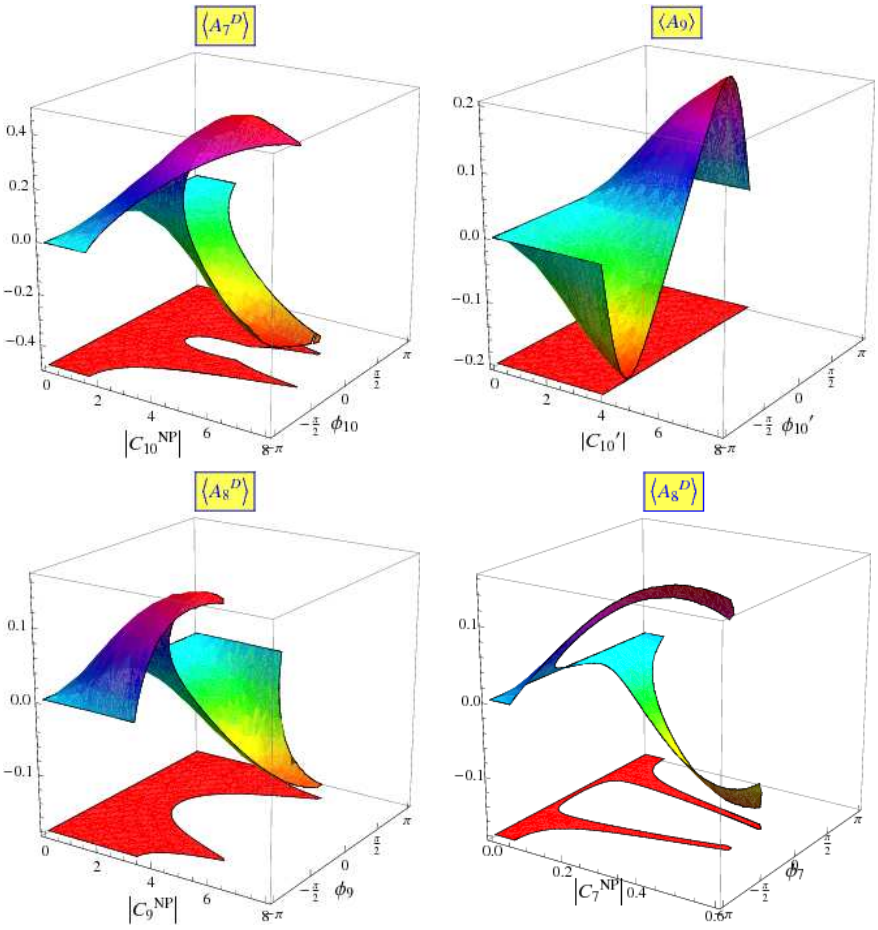

Figure 3: The dependence of the integrated T-odd CP asymmetries $\langle A_{7,8,9}^{(D)} \rangle$ for $(q^2_{\rm min}, q^2_{\rm max}) = (1, 6)$ GeV^2 on NP Wilson coefficients after applying the experimental constraints. In each plot all other NP Wilson coefficients have been set to zero.

In table 4 we show the allowed ranges of the CP asymmetries in various NP scenarios. Numerically we find that the CP asymmetries can deviate significantly from their SM values, which are doubly Cabibbo-suppressed and below the percent level. As anticipated, the T-even CP asymmetries can be enhanced by one order of magnitude up to $\lesssim 10\%$. The T-odd CP asymmetries $A_{7,8,9}^{(D)}$ can receive even stronger NP enhancements, up to order one.

There is also some residual dependence in the $A_i^{(D)}$ on all NP Wilson coefficients from the normalization to the CP averaged decay rate. Hence, even though the numerator of some CP asymmetries is independent of a particular Wilson coefficient, the asymmetries can be modified from their respective SM values given in table 2. These small effects are included in table 4 whenever they are distinguishable from the SM at 1σ, otherwise called SM-like.

Also the purely leptonic decay $\bar{B}_s \to \bar{\mu}\mu$ has strong sensitivity to NP contributions in $\mathcal{O}_{10}$ and $\mathcal{O}'_{10}$ since $\mathcal{B}(\bar{B}_s \to \bar{\mu}\mu) \propto |C_{10} - C'_{10}|^2$, see, e.g., [22]. We find a possible enhancement of $\mathcal{B}(\bar{B}_s \to \bar{\mu}\mu)$ up to almost an order of magnitude in NP scenarios with

JHEP07(2008)106

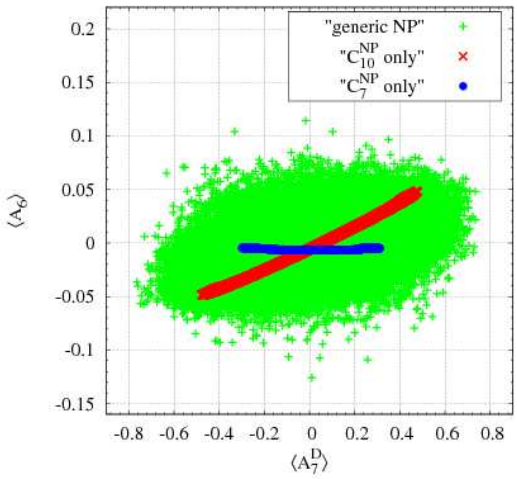

Figure 4: Correlations between the CP asymmetries $\langle A_7^D \rangle$ and $\langle A_6 \rangle$ in different scenarios of NP: generic NP, where all six coefficients are varied, and with NP in C_{10} and C_7 only.

these coefficients modified, see table 4. The largest branching ratio, obtained with generic NP, is still a factor of two below the current experimental upper bound given in table 3. Furthermore, $\mathcal{B}(\bar{B}_s \to \bar{\mu}\mu)$ can be suppressed with respect to the SM by cancellations between C_{10} and C'_{10}. A lower bound exists from data on the decays $B \to K^{(*)}\bar{l}l$, which are sensitive to $|C_{10} + C'_{10}|$ [22]. However, in models containing both $C_{10}^{\rm NP}$ and $C_{10}^{\prime\rm NP}$ only a very weak bound on $\mathcal{B}(\bar{B}_s \to \bar{\mu}\mu)$ can be obtained. We conclude that improved data on or a discovery of $\bar{B}_s \to \bar{\mu}\mu$ decays will have a strong impact on this type of analysis.

In figure 3 we show the dependence of the T-odd CP asymmetries $\langle A_{7,8,9}^{(D)} \rangle$ integrated over $(q^2_{\rm min}, q^2_{\rm max}) = (1, 6)$ GeV^2 on the NP Wilson coefficients as indicated. In the plots all other NP Wilson coefficients have been set to zero and the experimental FCNC constraints have been applied. The dependence of the asymmetries on the phases is very strong, making the CP asymmetries great probes of CP violation beyond the SM.

In figure 4 $\langle A_6 \rangle$ is shown against $\langle A_7^D \rangle$ for different NP scenarios. Both CP asymmetries are very sensitive to the phase of $C_{10}^{(\prime)}$, and A_7^D depends in addition on the dipole coefficients $C_7^{(\prime)}$. Correlations of this type can identify the nature of NP.

7. Summary

We exploited the full angular analysis in exclusive semileptonic $\bar{B} \to \bar{K}^*(\to \bar{K}\pi)\bar{l}l$ and $\bar{B}_s \to \phi(\to K^+K^-)\bar{l}l$ decays as a means of testing the SM and searching for new CP phases in $b \to s$ transitions. From the angular distributions in (2.1) and (2.5) seven CP asymmetries $A_{3\ldots9}^{(D)}$ in addition to the one in the decay rate can be accessed. We find that the SM predictions, valid for low dilepton masses, have rather large uncertainties $\sim 20\%$ for $A_{4,5}^D$, $\sim 50\%$ for $A_{\rm CP}, A_6, A_{7,8}^D$ and order one for $A_{3,9}$, but the tiny magnitude of the CP asymmetries $\lesssim 10^{-2}$ makes them all ideal to search for a variety of different NP effects.

JHEP07(2008)106

In particular, large NP effects are possible, which survive also the current experimental FCNC constraints. We summarize here specific features of the asymmetries:

- A_7^D, A_8^D, A_9 are T-odd and can be order one with New Physics.
- A_5^D, A_6, A_8^D, A_9 are CP-odd and can be obtained without tagging from $d\Gamma + d\bar{\Gamma}$.
- A_3, A_9 are very sensitive to right-handed currents.
- $A_3, A_9, (A_6)$ can be extracted from a single-differential distribution in $\phi(\theta_l)$.
- A_7^D is very sensitive to the phase of the Z-penguins $\sim C_{10}^{(\prime)}$.

Due to the CP-odd feature of some of the asymmetries and the width difference in the B_s-system, further CP asymmetries $A_i^{(D)mix}$ can be extracted from untagged, time-integrated $\bar{B}_s, B_s \to \phi(\to K^+K^-)\bar{l}l$ decays. In the presence of NP with large CP phases we expect order one (order ten percent) CP asymmetries related to the T-odd (T-even) asymmetries $A_{8,9}^{(D)mix}$ ($A_{5,6}^{(D)mix}$). The difference between the asymmetries originating from B_d- and B_s-decays is dominated by the difference in mixing.

A comparison of the B_d and B_s asymmetries hence probes the width difference and the mixing phase. One possibility is that the $A_i^{(D)mix}$ are order 10 percent, whereas $A_i^{(D)}$ are negligible, indicating that there is beyond-the-SM CP violation in $\Delta B = 2$ processes only. Note that a measurement of the $A_i^{(D)mix}$ is probably the only easy way to study CP violation in semileptonic rare $b \to s$ transitions with B_s-mesons.

We conclude that the CP asymmetries from the angular analysis map out precisely the CP properties of several Wilson coefficients. The minimal, that is, CKM description of CP violation can be disproved. This study can be extended to include also lepton flavor dependent effects along the lines of [42].

The prospects for studying rare dimuon modes at the LHC are promising: For an integrated luminosity of $2\, fb^{-1}$, i.e., after one nominal year of data taking, a few thousand $B_d \to K^{*0}\mu^+\mu^-$ events are expected at LHCb, allowing a measurement of the branching ratio and its CP asymmetry at the percent level [43]. The CP asymmetries proposed here require further information on angular distributions, thus higher statistics. A dedicated sensitivity study, also taking into account suitable cuts, would be desireable.

Acknowledgments

G.H. is happy to thank Frank Krüger for early discussions on A_7^D and Robert Fleischer for careful reading of the manuscript. C.B. would like to thank Sebastian Jäger for helpful explanations. The work by C.B. and G.H. is supported in part by the Bundesministerium für Bildung und Forschung, Berlin-Bonn. G.P. is supported by a grant from the G.I.F., the German-Israeli-Foundation for Scientific Research and Development. G.H. is grateful to the organizers and participants of the *Physics of the Large Hadron Collider*-workshop and acknowledges the hospitality and great research environment provided by the Kavli Institute for Theoretical Physics in Santa Barbara during the final phase of this work.

JHEP07(2008)106

A. Angular coefficients $J_i^{(a)}$

Here the functions $J_i^{(a)}$ in the angular distribution (2.1) are given in terms of the transversity amplitudes $A_{\perp,\parallel,0,t}$ [9]:

$$J_1^s = \frac{3}{4}\left\{\frac{(2+\beta_l^2)}{4}\left[|A_\perp^L|^2+|A_\parallel^L|^2+(L\to R)\right]+\frac{4m_l^2}{q^2}\mathrm{Re}\left(A_\perp^L A_\perp^{R*}+A_\parallel^L A_\parallel^{R*}\right)\right\}, \tag{A.1}$$

$$J_1^c = \frac{3}{4}\left\{|A_0^L|^2+|A_0^R|^2+\frac{4m_l^2}{q^2}\left[|A_t|^2+2\mathrm{Re}(A_0^L A_0^{R*})\right]\right\}, \tag{A.2}$$

$$J_2^s = \frac{3\beta_l^2}{16}\left[|A_\perp^L|^2+|A_\parallel^L|^2+(L\to R)\right], \tag{A.3}$$

$$J_2^c = -\frac{3\beta_l^2}{4}\left[|A_0^L|^2+(L\to R)\right], \tag{A.4}$$

$$J_3 = \frac{3}{8}\beta_l^2\left[|A_\perp^L|^2-|A_\parallel^L|^2+(L\to R)\right], \tag{A.5}$$

$$J_4 = \frac{3}{4\sqrt{2}}\beta_l^2\left[\mathrm{Re}(A_0^L A_\parallel^{L*})+(L\to R)\right], \tag{A.6}$$

$$J_5 = \frac{3\sqrt{2}}{4}\beta_l\left[\mathrm{Re}(A_0^L A_\perp^{L*})-(L\to R)\right], \tag{A.7}$$

$$J_6 = \frac{3}{2}\beta_l\left[\mathrm{Re}(A_\parallel^L A_\perp^{L*})-(L\to R)\right], \tag{A.8}$$

$$J_7 = \frac{3\sqrt{2}}{4}\beta_l\left[\mathrm{Im}(A_0^L A_\parallel^{L*})-(L\to R)\right], \tag{A.9}$$

$$J_8 = \frac{3}{4\sqrt{2}}\beta_l^2\left[\mathrm{Im}(A_0^L A_\perp^{L*})+(L\to R)\right], \tag{A.10}$$

$$J_9 = \frac{3}{4}\beta_l^2\left[\mathrm{Im}(A_\parallel^{L*} A_\perp^L)+(L\to R)\right], \tag{A.11}$$

where

$$\beta_l = \sqrt{1-\frac{4m_l^2}{q^2}}, \tag{A.12}$$

and the transversity amplitudes in QCDF can be seen in (C.5).

B. The effective Hamiltonian

We use the $\Delta B = 1$ effective Hamiltonian for $b\to s$ transitions, e.g., [44, 13]

$$\mathcal{H}_{\rm eff} = -\frac{4G_F}{\sqrt{2}}V_{tb}V_{ts}^*\left(\mathcal{H}_{\rm eff}^{(t)}+\hat{\lambda}_u\mathcal{H}_{\rm eff}^{(u)}\right), \qquad \hat{\lambda}_u = V_{ub}V_{us}^*/V_{tb}V_{ts}^*, \tag{B.1}$$

where V_{ij} denote CKM matrix elements and we used unitarity to write the basis as

$$\mathcal{H}_{\rm eff}^{(t)} = C_1\mathcal{O}_1^c + C_2\mathcal{O}_2^c + \sum_{i=3}^{10} C_i\mathcal{O}_i, \qquad \mathcal{H}_{\rm eff}^{(u)} = C_1(\mathcal{O}_1^c-\mathcal{O}_1^u)+C_2(\mathcal{O}_2^c-\mathcal{O}_2^u). \tag{B.2}$$

JHEP07(2008)106

Here, the $\mathcal{O}_{1,2}^{u,c}$ denote current-current operators whereas $\mathcal{O}_i$ for $i = 3,4,5,6$ are QCD-penguin operators, defined as in [45]. We further take into account the following dipole and semileptonic operators

$$\begin{aligned}
\mathcal{O}_7 &= \frac{e}{(4\pi)^2}\overline{m}_b[\bar{s}\sigma^{\mu\nu}P_R b]F_{\mu\nu}, & \mathcal{O}_7' &= \frac{e}{(4\pi)^2}\overline{m}_b[\bar{s}\sigma^{\mu\nu}P_L b]F_{\mu\nu},\\
\mathcal{O}_9 &= \frac{e^2}{(4\pi)^2}[\bar{s}\gamma_\mu P_L b][\bar{l}\gamma^\mu l], & \mathcal{O}_9' &= \frac{e^2}{(4\pi)^2}[\bar{s}\gamma_\mu P_R b][\bar{l}\gamma^\mu l],\\
\mathcal{O}_{10} &= \frac{e^2}{(4\pi)^2}[\bar{s}\gamma_\mu P_L b][\bar{l}\gamma^\mu\gamma_5 l], & \mathcal{O}_{10}' &= \frac{e^2}{(4\pi)^2}[\bar{s}\gamma_\mu P_R b][\bar{l}\gamma^\mu\gamma_5 l],
\end{aligned} \tag{B.3}$$

where $P_{R/L} = (1\pm\gamma_5)/2$ denote chiral projectors and $\overline{m}_b(\mu_b)$ is the $\overline{\rm MS}$ b-quark mass at the scale μ_b. Since in the SM $C_i' \sim m_s/m_b C_i$, the chirality flipped operators $\mathcal{O}_{7,9,10}'$ can only compete with $\mathcal{O}_{7,9,10}$ in models beyond the SM. The Wilson coefficients are decomposed into their SM and NP parts as $C_i = C_i^{\rm SM} + C_i^{\rm NP}$ and $C_i' = C_i'^{\rm NP}$ for $i = 7, 9, 10$.

C. Transversity amplitudes at NLO

Starting from the K^* transversity amplitudes $A_i(q^2)$, $i = \{\perp, \parallel, 0, t\}$ in naive factorization (see, e.g., [9]), the NLO α_s-corrections at large recoil using QCDF [12, 13] can be taken into account by the replacements [9, 10]

$$(C_7^{\rm eff} + C_7')T_i(q^2) \to \mathcal{T}_i^+, \qquad (C_7^{\rm eff} - C_7')T_i(q^2) \to \mathcal{T}_i^-, \qquad C_9^{\rm eff}(q^2) \to C_9, \tag{C.1}$$

where

$$\mathcal{T}_1^\pm = \mathcal{T}_\perp^\pm, \qquad \mathcal{T}_2^- = \frac{2E}{M_B}\mathcal{T}_\perp^-, \qquad \mathcal{T}_3^- = \mathcal{T}_\perp^- + \mathcal{T}_\parallel^-. \tag{C.2}$$

The functions $\mathcal{T}_{\perp,\parallel}^-$ can be obtained from the $\mathcal{T}_{\perp,\parallel}$ given in [12, 13] by substituting $C_7^{\rm eff}$ with $C_7^{\rm eff} - C_7'$ whereas $\mathcal{T}_\perp^+$ is obtained from $\mathcal{T}_\perp$ by replacing $C_7^{\rm eff}$ with $C_7^{\rm eff} + C_7'$.

In (C.1), the T_i, $i = 1,2,3$ denote the QCD tensor form factors defined in appendix E. The effective electroweak Hamiltonian employed is given in appendix B. The effective coefficients $C_{7,8}^{\rm eff}$ and $C_9^{\rm eff}(q^2)$ have been introduced to absorb 1-loop matrix elements of 4-quark operators [46]. Here, such contributions to $\mathcal{O}_9$ are contained in $\mathcal{T}_i^\pm$ together with further corrections beyond naive factorization. We take $C_7^{\rm eff}$ and $C_{9,10}$ at NNLL in the SM at the scale μ_b. In the NP scenarios discussed in this work, $C_7'^{\rm eff}$ equals C_7'.

In the framework of QCDF, the functions $\mathcal{T}_{\perp,\parallel}^\pm$ are known at NLO in α_s for the SM operators and the corresponding chirality flipped operators, see (B.3). The $\mathcal{T}_{\perp,\parallel}^\pm$ have the following CKM and QCD structure

$$\begin{aligned}
\mathcal{T}_a^\pm &= \mathcal{T}_a^{\pm(t)} + \hat{\lambda}_u \mathcal{T}_a^{(u)},\\
\mathcal{T}_a^{\pm(t)} &= \mathcal{T}_a^{\pm(t),{\rm LO}} + \frac{\alpha_s}{4\pi}\mathcal{T}_a^{\pm(t),{\rm NLO}}, \qquad \mathcal{T}_a^{(u)} = \mathcal{T}_a^{(u),{\rm LO}} + \frac{\alpha_s}{4\pi}\mathcal{T}_a^{(u),{\rm NLO}},
\end{aligned} \tag{C.3}$$

where $a = \perp, \parallel$. At LO in α_s (denoted by the superscript (0)) they read

$$\mathcal{T}_\perp^{\pm(t),\mathrm{LO}} = \xi_\perp \left[C_7^{\mathrm{eff}(0)} \pm C_7^{\prime(0)} + \frac{q^2}{2m_b M_B} Y^{(0)} \right], \qquad \mathcal{T}_\perp^{(u),\mathrm{LO}} = \xi_\perp \frac{q^2}{2m_b M_B} Y^{(u)(0)}, \quad \text{(C.4)}$$
$$\mathcal{T}_\parallel^{-(t),\mathrm{LO}} = -\xi_\parallel \left[C_7^{\mathrm{eff}(0)} - C_7^{\prime(0)} + \frac{M_B}{2m_b} Y^{(0)} \right] + HS, \quad \mathcal{T}_\parallel^{(u),\mathrm{LO}} = -\xi_\parallel \frac{M_B}{2m_b} Y^{(u)(0)} + HS,$$

where $Y(q^2)$ and $Y^{(u)}(q^2)$ contain 1-loop contributions of four-quark operators $\sim \bar{s}b\bar{q}q$ with an imaginary part for $q^2 > 4m_q^2$. Since the charm threshold is at the very upper end - if not outside - the q^2-region where the $1/E$ expansion works and the lighter quarks induce either CKM suppressed or penguin contributions, the resulting strong phase is small. In (C.4), spectator effects are denoted by HS. At lowest order, these are in $\mathcal{T}_\parallel^{(u),\mathrm{LO}}$ and $\mathcal{T}_\parallel^{-(t),\mathrm{LO}}$. The latter is suppressed by penguin coefficients, whereas the former is non-zero only for charged $B^\pm \to K^{*\pm}\bar{l}l$ decays (weak annihilation). At higher order in α_s, strong phases are further generated in $\mathcal{T}_a^{(i),\mathrm{NLO}}$ and from spectator interactions [12, 13], which have been included in our numerical analysis. The form factors $\xi_\perp$ and $\xi_\parallel$ are discussed in appendix E.

The transversity amplitudes in the presence of NP Wilson coefficients within QCDF and neglecting kinematical terms[2] $M_{K^*}^2/M_B^2$ read as

$$\begin{aligned}
A_\perp^{L,R} &= +\sqrt{2} N M_B (1-\hat{s}) \left\{ \Big[(C_9 + C_9') \mp (C_{10} + C_{10}') \Big] \xi_\perp + \frac{2\hat{m}_b}{\hat{s}} \mathcal{T}_\perp^+ \right\}, \\
A_\parallel^{L,R} &= -\sqrt{2} N M_B (1-\hat{s}) \left\{ \Big[(C_9 - C_9') \mp (C_{10} - C_{10}') \Big] \xi_\perp + \frac{2\hat{m}_b}{\hat{s}} \mathcal{T}_\perp^- \right\}, \\
A_0^{L,R} &= -\frac{N M_B^2 (1-\hat{s})^2}{2 M_{K^*} \sqrt{\hat{s}}} \left\{ \Big[(C_9 - C_9') \mp (C_{10} - C_{10}') \Big] \xi_\parallel - 2\hat{m}_b \mathcal{T}_\parallel^- \right\}, \\
A_t &= \frac{N M_B^2 (1-\hat{s})^2}{M_{K^*} \sqrt{\hat{s}}} (C_{10} - C_{10}') \frac{\xi_\parallel}{\Delta_\parallel},
\end{aligned} \quad \text{(C.5)}$$

where

$$\hat{s} = \frac{q^2}{M_B^2}, \qquad \hat{m}_b = \frac{m_b}{M_B}, \qquad N = \left[\frac{G_F^2 \alpha_e^2}{3 \cdot 2^{10} \pi^5 M_B} |V_{tb} V_{ts}^*|^2 \, \hat{s} \, \sqrt{\lambda} \, \beta_l \right]^{1/2} \quad \text{(C.6)}$$

and $\lambda = M_B^4 + M_{K^*}^4 + q^4 - 2(M_B^2 M_{K^*}^2 + M_B^2 q^2 + M_{K^*}^2 q^2)$. Note that A_t contributes only for $m_l \neq 0$ and contains $\Delta_\parallel$, see [12], which represents form factor symmetry breaking QCD corrections. Note that helicity conservation dictates $A_\perp^{L,R} = -A_\parallel^{L,R}$ for $C_i' = 0$ up to $1/E$ corrections [47].

The dilepton spectrum defined in (2.7) can be written in terms of the transversity amplitudes (C.5) as

$$\frac{d\Gamma}{dq^2} = |A_\perp^L|^2 + |A_\parallel^L|^2 + |A_0^L|^2 + (L \to R) + \mathcal{O}\left(m_l^2/q^2\right) \quad \text{(C.7)}$$

[2]These formally subleading terms in the $1/E$ expansion are included in the numerical evaluation.

JHEP07(2008)106

up to contributions suppressed by the lepton mass. The dependence on the form factors stems from $\xi_\perp$ for $A_\perp^{L,R}, A_\parallel^{L,R}$ and $\xi_\parallel$ for $A_0^{L,R}$. Since the longitudinal amplitudes $A_0^{L,R}$ are enhanced by M_B/M_{K^*}, see (C.5), they imply a stronger dependence of $d\Gamma/dq^2$ on $\xi_\parallel$ than on $\xi_\perp$. Quantitatively, we find in the SM that for the cuts $(q^2_{\rm min}, q^2_{\rm max}) = (1,6)$ GeV^2 and $(1,7)$ GeV^2 the contribution from the longitudinal K^* to the total decay rate,

$$\mathcal{F}_L = \frac{\langle |A_0^L|^2 + |A_0^R|^2 \rangle}{\langle d\Gamma/dq^2 \rangle}, \tag{C.8}$$

is $0.73^{+0.08}_{-0.10}$ and $0.72^{+0.08}_{-0.11}$, respectively.

D. CP asymmetries and $A_{\rm FB}$ beyond the SM

Here we give analytical expressions of the CP asymmetries defined in (3.2) and (3.3) including contributions from NP operators (B.3). The asymmetries have been obtained from the transversity amplitudes in QCDF, see (C.5), valid in the low dilepton mass region. The coefficients $C_7^{\rm eff} = C_7^{\rm eff,SM} + C_7^{\rm NP}$ and C_7' are taken into account by $\mathcal{T}^\pm_{\perp,\parallel}$. Except for $A_{\rm CP}$, the CP asymmetries are given with their full lepton mass dependence which is confined to powers of β_l. Neglecting kinematical factors $M_{K^*}^2/M_B^2$, the CP asymmetries as a function of the dilepton mass can be written as

$$A_{\rm CP} = \mathcal{A}\frac{8\hat{m}_b}{3\hat{s}}{\rm Re}\Bigg\{\frac{\xi_\parallel^2}{\xi_\perp^2}\frac{M_B^2}{M_{K^*}^2}\frac{(1-\hat{s})^2}{8}\left[\hat{m}_b\frac{|\mathcal{T}_\parallel^-|^2}{\xi_\parallel^2} - \frac{\mathcal{T}_\parallel^-}{\xi_\parallel}(C_9 - C_9')^*\right] + \frac{\hat{m}_b}{\hat{s}}\frac{|\mathcal{T}_\perp^+|^2 + |\mathcal{T}_\perp^-|^2}{\xi_\perp^2} + \frac{\mathcal{T}_\perp^+ - \mathcal{T}_\perp^-}{\xi_\perp}C_9^* + \frac{\mathcal{T}_\perp^+ + \mathcal{T}_\perp^-}{\xi_\perp}C_9'^* - (\delta_W \to -\delta_W)\Bigg\} + \mathcal{O}\left(m_l^2/q^2\right), \tag{D.1}$$

$$A_3 = \mathcal{A}\frac{2\hat{m}_b\beta_l}{\hat{s}}{\rm Re}\Bigg\{\frac{\hat{m}_b}{\hat{s}}\frac{|\mathcal{T}_\perp^+|^2 - |\mathcal{T}_\perp^-|^2}{\xi_\perp^2} + \frac{\mathcal{T}_\perp^+ - \mathcal{T}_\perp^-}{\xi_\perp}C_9^* + \frac{\mathcal{T}_\perp^+ + \mathcal{T}_\perp^-}{\xi_\perp}C_9'^* - (\delta_W \to -\delta_W)\Bigg\}, \tag{D.2}$$

$$A_4^D = -\mathcal{A}^D\frac{\hat{m}_b\beta_l}{2\hat{s}}{\rm Re}\Bigg\{\left(\frac{\mathcal{T}_\perp^-}{\xi_\perp} - \hat{s}\frac{\mathcal{T}_\parallel^-}{\xi_\parallel}\right)(C_9 - C_9')^* - 2\hat{m}_b\frac{\mathcal{T}_\perp^-(\mathcal{T}_\parallel^-)^*}{\xi_\perp\xi_\parallel} - (\delta_W \to -\delta_W)\Bigg\}, \tag{D.3}$$

$$A_5^D = -\mathcal{A}^D\frac{\hat{m}_b}{\hat{s}}{\rm Re}\Bigg\{\left(\frac{\mathcal{T}_\perp^-}{\xi_\perp} - \hat{s}\frac{\mathcal{T}_\parallel^-}{\xi_\parallel}\right)C_{10} - \left(\frac{\mathcal{T}_\perp^-}{\xi_\perp} + \hat{s}\frac{\mathcal{T}_\parallel^-}{\xi_\parallel}\right)C_{10}'^* - (\delta_W \to -\delta_W)\Bigg\}, \tag{D.4}$$

$$A_6 = \mathcal{A}\frac{4\hat{m}_b}{\hat{s}}{\rm Re}\Bigg\{\frac{\mathcal{T}_\perp^+ + \mathcal{T}_\perp^-}{\xi_\perp}C_{10}^* - \frac{\mathcal{T}_\perp^+ - \mathcal{T}_\perp^-}{\xi_\perp}C_{10}'^* - (\delta_W \to -\delta_W)\Bigg\}, \tag{D.5}$$

$$A_7^D = \mathcal{A}^D\frac{\hat{m}_b}{\hat{s}}{\rm Im}\Bigg\{(C_{10} - C_{10}')\left(\frac{\mathcal{T}_\perp^-}{\xi_\perp} + \hat{s}\frac{\mathcal{T}_\parallel^-}{\xi_\parallel}\right)^* - (\delta_W \to -\delta_W)\Bigg\}, \tag{D.6}$$

$$A_8^D = \mathcal{A}^D\frac{\beta_l}{2}\,{\rm Im}\Bigg\{\frac{2\hat{m}_b^2}{\hat{s}}\frac{\mathcal{T}_\perp^+(\mathcal{T}_\parallel^-)^*}{\xi_\perp\xi_\parallel} - \frac{\hat{m}_b}{\hat{s}}\left[\left(\frac{\mathcal{T}_\perp^+}{\xi_\perp} + \hat{s}\frac{\mathcal{T}_\parallel^-}{\xi_\parallel}\right)C_9^* - \left(\frac{\mathcal{T}_\perp^+}{\xi_\perp} - \hat{s}\frac{\mathcal{T}_\parallel^-}{\xi_\parallel}\right)C_9'^*\right] + C_9C_9'^* + C_{10}C_{10}'^* - (\delta_W \to -\delta_W)\Bigg\}, \tag{D.7}$$

$$A_9 = -\mathcal{A}\,2\beta_l \mathrm{Im}\Big\{ \frac{2\hat{m}_b^2}{\hat{s}^2}\frac{\mathcal{T}_\perp^+(\mathcal{T}_\perp^-)^*}{\xi_\perp^2} + \frac{\hat{m}_b}{\hat{s}}\left[\frac{\mathcal{T}_\perp^+ - \mathcal{T}_\perp^-}{\xi_\perp}C_9^* - \frac{\mathcal{T}_\perp^+ + \mathcal{T}_\perp^-}{\xi_\perp}C_9'^*\right] - C_9 C_9'^* - C_{10}C_{10}'^* - (\delta_W \to -\delta_W)\Big\}, \tag{D.8}$$

where $(\delta_W \to -\delta_W)$ is short hand notation for conjugating all weak phases. Furthermore,

$$\mathcal{A} = \frac{G_F^2\,\alpha_e^2}{3^2\cdot 2^6\,\pi^5}|V_{tb}V_{ts}^*|^2\frac{M_B^3\beta_l^2\hat{s}(1-\hat{s})^3\xi_\perp^2}{N_\Gamma},$$
$$\mathcal{A}^D = \frac{G_F^2\,\alpha_e^2}{3^2\cdot 2^6\,\pi^5}|V_{tb}V_{ts}^*|^2\frac{M_B^4\beta_l^2\sqrt{\hat{s}}(1-\hat{s})^4\xi_\parallel\xi_\perp}{M_{K^*}N_\Gamma}, \tag{D.9}$$

where N_Γ is defined in (3.2).

At lowest order in α_s, the expressions for the above CP asymmetries simplify by

$$\frac{\mathcal{T}_\perp^{+,\mathrm{LO}} - \mathcal{T}_\perp^{-,\mathrm{LO}}}{\xi_\perp} = 2C_7^{\prime(0)}, \tag{D.10}$$

$$\frac{\mathcal{T}_\perp^{+,\mathrm{LO}} + \mathcal{T}_\perp^{-,\mathrm{LO}}}{\xi_\perp} = 2C_7^{\mathrm{eff}(0)} + \frac{\hat{s}}{\hat{m}_b}(Y^{(0)} + \hat{\lambda}_u Y^{(u)(0)}), \tag{D.11}$$

$$\frac{\mathcal{T}_\perp^{\pm,\mathrm{LO}}}{\xi_\perp} + \hat{s}\frac{\mathcal{T}_\parallel^{-,\mathrm{LO}}}{\xi_\parallel} = \begin{cases} (1-\hat{s})C_7^{\mathrm{eff}(0)} + (1+\hat{s})C_7^{\prime(0)} \\ (1-\hat{s})(C_7^{\mathrm{eff}(0)} - C_7^{\prime(0)}) \end{cases}. \tag{D.12}$$

Note that in the SM, or more general, in any model without right-handed contributions to the electromagnetic dipole operator, $\mathcal{T}_\perp^+ = \mathcal{T}_\perp^-$, see appendix C.

The lepton forward-backward asymmetry in QCDF is written as

$$A_{\mathrm{FB}} = \frac{12\beta_l N^2 M_B^2(1-\hat{s})^2\xi_\perp^2}{d\Gamma/dq^2} \times \mathrm{Re}\Big\{\left[C_9 + \frac{\hat{m}_b}{\hat{s}}\frac{(\mathcal{T}_\perp^+ + \mathcal{T}_\perp^-)}{\xi_\perp}\right]C_{10}^* - \left[C_9' + \frac{\hat{m}_b}{\hat{s}}\frac{(\mathcal{T}_\perp^+ - \mathcal{T}_\perp^-)}{\xi_\perp}\right]C_{10}'^*\Big\}. \tag{D.13}$$

E. $B \to K^*$ form factors at large recoil

The $B \to K^*$ matrix element can be parametrized in terms of seven q^2-dependent QCD form factors $V, A_{0,1,2}$ and $T_{1,2,3}$ as

$$\langle K^*(p_B-q)|\bar{s}\gamma_\mu(1-\gamma_5)b|B(p_B)\rangle = -2\epsilon_{\mu\nu\alpha\beta}\varepsilon^{*\nu}p_B^\alpha q^\beta\frac{V}{M_B+M_{K^*}} - i\varepsilon_\mu^*(M_B+M_{K^*})A_1 + i(2p_B-q)_\mu(\varepsilon^*\cdot q)\frac{A_2}{M_B+M_{K^*}} + iq_\mu(\varepsilon^*\cdot q)\frac{2M_{K^*}}{q^2}[A_3-A_0], \tag{E.1}$$

$$\langle K^*(p_B-q)|\bar{s}\sigma_{\mu\nu}q^\nu(1+\gamma_5)b|B(p_B)\rangle = -2i\,\epsilon_{\mu\nu\alpha\beta}\varepsilon^{*\nu}p_B^\alpha q^\beta\,T_1 + [\varepsilon_\mu^*(M_B^2-M_{K^*}^2) - (\varepsilon^*\cdot q)(2p_B-q)_\mu]\,T_2 + (\varepsilon^*\cdot q)\left[q_\mu - \frac{q^2}{M_B^2-M_{K^*}^2}(2p_B-q)_\mu\right]T_3 \tag{E.2}$$

	r_1	r_2	m_R^2 [GeV^2]	$m_{\rm fit}^2$ [GeV^2]	$F(0)$	$\Delta_0 F(0)$	$\Delta_{a_1} F(0)$
V	0.923	-0.511	5.32^2	49.40	0.411	0.033	$0.44\delta_{a_1}$
A_1		0.290		40.38	0.292	0.028	$0.33\delta_{a_1}$
A_2	-0.084	0.342		52.00	0.259	0.027	$0.31\delta_{a_1}$

Table 5: The parameters $r_{1,2}, m_R^2$ and $m_{\rm fit}^2$ describing the q^2 dependence of the form factors V and $A_{1,2}$ in the LCSR approach [25]. Also shown are the corresponding values of the form factors at $q^2 = 0$, $F(0)$, their uncertainties independent of the Gegenbauer moment a_{1,K^*}, $\Delta_0 F(0)$ and the uncertainties induced by a_{1,K^*} in terms of $\delta_{a_1} = (a_{1,K^*}(1\text{ GeV}) - 0.1)$, $\Delta_{a_1} F(0)$.

and

$$A_3 = \frac{M_B + M_{K^*}}{2M_{K^*}} A_1 - \frac{M_B - M_{K^*}}{2M_{K^*}} A_2, \tag{E.3}$$

where $\epsilon^{*\mu}$ denotes the polarization vector of the K^* and p_B^μ the four momentum of the B meson. The QCD form factors obey symmetry relations in the large recoil limit and can be expressed at leading order in the $1/E$ expansion in terms of two universal form factors $\xi_\perp$ and $\xi_\parallel$ [11]. Symmetry breaking corrections at order α_s have been calculated using QCDF in ref. [48]. We employ a factorization scheme within QCDF where the $\xi_{\perp,\parallel}$ are related to the $V, A_{1,2}$ as [13]

$$\xi_\perp = \frac{M_B}{M_B + M_{K^*}} V, \qquad \xi_\parallel = \frac{M_B + M_{K^*}}{2E} A_1 - \frac{M_B - M_{K^*}}{M_B} A_2. \tag{E.4}$$

For the q^2 dependence of the universal form factors we adopt the findings from light cone sum rule (LCSR) calculations [25]. Here the q^2 dependence is parametrized as

$$V(q^2) = \frac{r_1}{1 - q^2/m_R^2} + \frac{r_2}{1 - q^2/m_{\rm fit}^2}, \tag{E.5}$$

$$A_1(q^2) = \frac{r_2}{1 - q^2/m_{\rm fit}^2}, \tag{E.6}$$

$$A_2(q^2) = \frac{r_1}{1 - q^2/m_{\rm fit}^2} + \frac{r_2}{(1 - q^2/m_{\rm fit}^2)^2}, \tag{E.7}$$

where the fit parameters $r_{1,2}, m_R^2$ and $m_{\rm fit}^2$ are shown in table 5. Also given in this table are the values of the form factors at $q^2 = 0$ and the corresponding parametric uncertainties within the LCSR approach. We give the uncertainties independent of the Gegenbauer moments $a_{1,K^*}^{\perp,\parallel}$ and the ones due to $a_{1,K^*}^{\perp,\parallel}$ separately. The relative uncertainty of the form factors $V(0), A_1(0)$ and $A_2(0)$ amounts to 8%, 10% and 10% without, and 11%, 12% and 14% after adding the a_{1,K^*} — see table 1 for the numerical value — induced uncertainty in quadrature, respectively. We use the total relative uncertainty from maximal recoil as an estimate for the form factor uncertainties for $q^2 > 0$. The form factors $\xi_{\perp,\parallel}$ defined via (E.4) are shown as a function of q^2 in figure 5. Here the bands indicate the uncertainty in $\xi_\perp$ and $\xi_\parallel$ of 11% and 14%, respectively.

F. Model-independent CP asymmetries beyond the SM

We give numerical formulae for the q^2-integrated quantities $\mathcal{B} = \tau_{B^0} \langle d\Gamma/dq^2 \rangle$, $\overline{\mathcal{B}} = \tau_{B^0} \langle d\bar{\Gamma}/dq^2 \rangle$ and $\text{Num} \left\langle A_i^{(D)} \right\rangle$ for $q^2 \in [1, 6]$ GeV^2 in terms of the NP Wilson coefficients

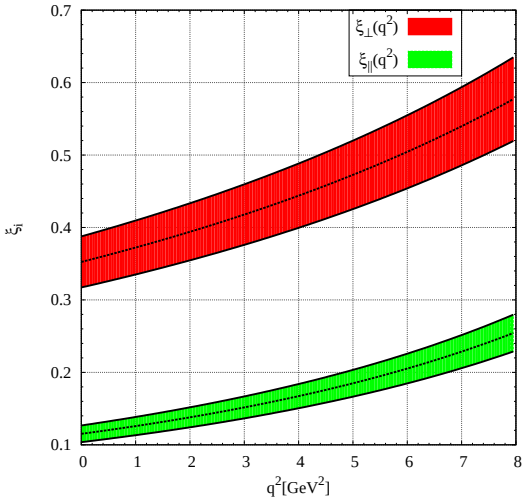

Figure 5: The universal form factors $\xi_\perp$ and $\xi_\parallel$ in the low-q^2 region and their uncertainty indicated by the bands.

$C_i^{\rm NP}$. Here, Num $\left\langle A_i^{(D)}\right\rangle$ denotes the numerators of the CP asymmetries multiplied by the B-meson lifetime such that the normalized CP asymmetries (see (3.5)) are obtained from

$$\left\langle A_i^{(D)}\right\rangle = \frac{\text{Num}\left\langle A_i^{(D)}\right\rangle}{\mathcal{B}+\overline{\mathcal{B}}}. \tag{F.1}$$

The dependence of the branching ratios on the NP Wilson coefficients can be written as

$$X = X_{\rm SM}\left[1+\sum_i\left(a_i|C_i^{\rm NP}|^2+b_i{\rm Re}C_i^{\rm NP}+c_i{\rm Im}C_i^{\rm NP}\right)+\sum_{j>i}d_{ij}{\rm Re}(C_i^{\rm NP}C_j^{\rm NP*})\right] \quad \text{for } \mathcal{B},\overline{\mathcal{B}}, \tag{F.2}$$

whereas the numerators of the T-odd CP asymmetries are parametrized as

$$X = X_{\rm SM}\left[1+\sum_i\left(b_i{\rm Re}C_i^{\rm NP}+c_i{\rm Im}C_i^{\rm NP}\right)+\sum_{j>i}e_{ij}{\rm Im}(C_i^{\rm NP}C_j^{\rm NP*})\right] \quad \text{for Num}\left\langle A_{7,8}^D\right\rangle. \tag{F.3}$$

The numerators of the T-even CP asymmetries read as

$$X = X_{\rm SM}\left[1+\sum_i\left(b_i{\rm Re}C_i^{\rm NP}+c_i{\rm Im}C_i^{\rm NP}\right)\right] \quad \text{for Num}\left\langle A_{\rm CP,6}\right\rangle, \text{Num}\left\langle A_{4,5}^D\right\rangle. \tag{F.4}$$

Here, the summations are over $i,j=7,7',9,9',10,10'$ and $X_{\rm SM}$ denotes the SM prediction of the corresponding quantity. Note that for Num$\langle A_{3,9}\rangle$ we have set $X_{\rm SM}$ to zero, see section 5, and, hence, the corresponding formulae read as

$$X = \sum_i\left(b_i{\rm Re}C_i^{\rm NP}+c_i{\rm Im}C_i^{\rm NP}\right) \quad \text{for Num}\left\langle A_3\right\rangle, \tag{F.5}$$

$$X = \sum_i\left(b_i{\rm Re}C_i^{\rm NP}+c_i{\rm Im}C_i^{\rm NP}\right)+\sum_{j>i}e_{ij}{\rm Im}(C_i^{\rm NP}C_j^{\rm NP*}) \quad \text{for Num}\left\langle A_9\right\rangle. \tag{F.6}$$

JHEP07(2008)106

$X_{\rm SM}$		$i=7$	$i=7'$	$i=9$	$i=9'$	$i=10$	$i=10'$
$\mathcal{B}_{\rm SM}$	a_i	2.634	2.634	0.035	0.035	0.035	0.035
	b_i	−0.271	−0.373	0.162	−0.179	−0.288	0.205
$= 2.444 \cdot 10^{-7}$	c_i	−0.156	0.001	−0.009	−0.0002	0	0
$\overline{\mathcal{B}}_{\rm SM}$	a_i	2.656	2.656	0.036	0.036	0.035	0.035
	b_i	−0.312	−0.370	0.158	−0.178	−0.290	0.206
$= 2.423 \cdot 10^{-7}$	c_i	0.106	0.003	0.004	0.002	0	0
$\mathrm{Num}\,\langle A_{\rm CP}\rangle_{\rm SM}$	b_i	4.469	−0.726	0.587	−0.345	0	0
$= 2.068 \cdot 10^{-9}$	c_i	−30.770	−0.275	−1.500	−0.259	0	0
$\mathrm{Num}\,\langle A_3\rangle_{\rm SM}$	b_i	−0.077	5.720	−0.012	0.378	0	0
$= 0^\dagger$	c_i	0.542	−47.174	0.081	−2.743	0	0
$\mathrm{Num}\,\langle A_4^D\rangle_{\rm SM}$	b_i	3.604	−3.604	0.536	−0.536	0	0
$= -8.642 \cdot 10^{-10}$	c_i	−1.435	1.435	−2.487	2.487	0	0
$\mathrm{Num}\,\langle A_5^D\rangle_{\rm SM}$	b_i	0	0	0	0	−0.244	0.068
$= 3.718 \cdot 10^{-9}$	c_i	0	0	0	0	1.152	−1.258
$\mathrm{Num}\,\langle A_6\rangle_{\rm SM}$	b_i	0	0	0	0	−0.244	0.004
$= -3.117 \cdot 10^{-9}$	c_i	0	0	0	0	1.774	−0.026
$\mathrm{Num}\,\langle A_7^D\rangle_{\rm SM}$	b_i	0	0	0	0	−0.244	0.244
$= -2.496 \cdot 10^{-9}$	c_i	−247.248	247.248	0	0	23.019	−23.019
$\mathrm{Num}\,\langle A_8^D\rangle_{\rm SM}$	b_i	−0.491	−1.423	0.176	−0.288	0	0
$= 1.706 \cdot 10^{-9}$	c_i	−189.333	−170.364	−16.524	−7.160	0	26.834
$\mathrm{Num}\,\langle A_9\rangle_{\rm SM}$	b_i	0	−8.390	0.007	−0.491	0	0
$= 0^\dagger$	c_i	−6.514	225.487	−0.568	6.064	0	31.913

Table 6: The SM predictions $X_{\rm SM}$ and the corresponding coefficients a_i, b_i and c_i for $i = 7, 7', 9, 9', 10, 10'$. †For $\mathrm{Num}\,\langle A_{3,9}\rangle$ $X_{\rm SM}$ has been set to zero and the corresponding coefficients are given in units of 10^{-9}.

d_{ij}	$\mathcal{B}$	$\overline{\mathcal{B}}$	e_{ij}	$\mathrm{Num}\,\langle A_7^D\rangle$	$\mathrm{Num}\,\langle A_8^D\rangle$	$\mathrm{Num}\,\langle A_9\rangle^\dagger$
$7,7'$	−0.255	−0.257	$7,7'$	0	200.542	1801.269
$7,9$	0.394	0.397	$7,9$	0	−43.413	−1.547
$7,9'$	−0.107	−0.108	$7,9'$	0	56.532	105.869
$7,10$	0	0	$7,10$	60.420	0	0
$7,10'$	0	0	$7,10'$	−60.420	0	0
$7',9$	−0.107	−0.108	$7',9$	0	−56.532	−105.869
$7',9'$	0.394	0.397	$7',9'$	0	43.413	1.547
$7',10$	0	0	$7',10$	−60.420	0	0
$7',10'$	0	0	$7',10'$	60.420	0	0
$9,9'$	−0.050	−0.050	$9,9'$	0	6.558	7.799
$10,10'$	−0.050	−0.050	$10,10'$	0	6.558	7.799

Table 7: The coefficients d_{ij} and e_{ij} for $i, j = 7, 7', 9, 9', 10, 10'$ and $j > i$. †For $\mathrm{Num}\,\langle A_9\rangle$ $X_{\rm SM}$ has been set to zero and the corresponding coefficients are given in units of 10^{-9}.

The SM predictions $X_{\rm SM}$ and the coefficients a_i, b_i, c_i and d_{ij}, e_{ij} are given in table 6 and table 7, respectively. We assumed central values for all parameters.

JHEP07(2008)106

References

[1] S. Hashimoto et al., *Letter of intent for KEK super B factory*, KEK-REPORT-2004-4;
J.L. Hewett et al., *The discovery potential of a super B factory*, Proceedings of *SLAC Workshops*, Stanford U.S.A. 2003 [hep-ph/0503261];
M. Bona et al., *SuperB: a high-luminosity asymmetric e^+e^- super flavor factory*, arXiv:0709.0451;
M. Artuso et al., *B, D and K decays*, arXiv:0801.1833;
T.E. Browder, T. Gershon, D. Pirjol, A. Soni and J. Zupan, *New physics at a super flavor factory*, arXiv:0802.3201.

[2] CDF collaboration, T. Aaltonen et al., *First flavor-tagged determination of bounds on mixing-induced CP-violation in $B_s \to J/\psi\phi$ decays*, *Phys. Rev. Lett.* **100** (2008) 161802 [arXiv:0712.2397];
D0 collaboration, V.M. Abazov et al., *Measurement of B_s^0 mixing parameters from the flavor-tagged decay $B_s^0 \to J/\psi\phi$*, arXiv:0802.2255.

[3] Heavy Flavor Averaging Group (HFAG) collaboration, E. Barberio et al., *Averages of b-hadron properties at the end of* 2005, hep-ex/0603003.

[4] Belle collaboration, K. Abe et al., *Measurement of the differential Q^2 spectrum and forward-backward asymmetry for $B \to K^*\ell^+\ell^-$*, hep-ex/0410006.

[5] A. Ishikawa et al., *Measurement of forward-backward asymmetry and Wilson coefficients in $B \to K^*\ell^+\ell^-$*, *Phys. Rev. Lett.* **96** (2006) 251801 [hep-ex/0603018].

[6] BABAR collaboration, B. Aubert et al., *Measurements of branching fractions, rate asymmetries and angular distributions in the rare decays $B \to K\ell^+\ell^-$ and $B \to K^*\ell^+\ell^-$*, *Phys. Rev.* **D 73** (2006) 092001 [hep-ex/0604007]; *Angular distributions in the decays $B \to K^*\ell^+\ell^-$*, arXiv:0804.4412.

[7] F. Krüger, L.M. Sehgal, N. Sinha and R. Sinha, *Angular distribution and CP asymmetries in the decays $\bar{B} \to K^-\pi^+e^-e^+$ and $\bar{B} \to \pi^-\pi^+e^-e^+$*, *Phys. Rev.* **D 61** (2000) 114028 [*Erratum ibid.* **D 63** (2001) 019901] [hep-ph/9907386].

[8] D. Melikhov, N. Nikitin and S. Simula, *Probing right-handed currents in $B \to K^*\ell^+\ell^-$ transitions*, *Phys. Lett.* **B 442** (1998) 381 [hep-ph/9807464];
C.S. Kim, Y.G. Kim, C.-D. Lu and T. Morozumi, *Azimuthal angle distribution in $B \to K^*(\to K\pi)\ell^+\ell^-$ at low invariant $m(\ell^+\ell^-)$ region*, *Phys. Rev.* **D 62** (2000) 034013 [hep-ph/0001151];
C.S. Kim, Y.G. Kim and C.-D. Lu, *Possible supersymmetric effects on angular distributions in $B \to K^*(\to K\pi)\ell^+\ell^-$ decays*, *Phys. Rev.* **D 64** (2001) 094014 [hep-ph/0102168].

[9] F. Krüger and J. Matias, *Probing new physics via the transverse amplitudes of $B^0 \to K^{*0}(\to K^-\pi^+)\ell^+\ell^-$ at large recoil*, *Phys. Rev.* **D 71** (2005) 094009 [hep-ph/0502060].

[10] E. Lunghi and J. Matias, *Huge right-handed current effects in $B \to K^*(K\pi)\ell^+\ell^-$ in supersymmetry*, *JHEP* **04** (2007) 058 [hep-ph/0612166].

[11] J. Charles, A. Le Yaouanc, L. Oliver, O. Pene and J.C. Raynal, *Heavy-to-light form factors in the heavy mass to large energy limit of QCD*, *Phys. Rev.* **D 60** (1999) 014001 [hep-ph/9812358].

[12] M. Beneke, T. Feldmann and D. Seidel, *Systematic approach to exclusive $B \to V\ell^+\ell^-, V\gamma$ decays*, *Nucl. Phys.* **B 612** (2001) 25 [hep-ph/0106067].

JHEP07(2008)106

[13] M. Beneke, T. Feldmann and D. Seidel, *Exclusive radiative and electroweak $b \to d$ and $b \to s$ penguin decays at NLO*, *Eur. Phys. J.* **C 41** (2005) 173 [hep-ph/0412400].

[14] A. Ali, G. Kramer and G.-H. Zhu, *$B \to K^* \ell^+ \ell^-$ in soft-collinear effective theory*, *Eur. Phys. J.* **C 47** (2006) 625 [hep-ph/0601034];
K.S.M. Lee, Z. Ligeti, I.W. Stewart and F.J. Tackmann, *Extracting short distance information from $b \to s\ell^+\ell^-$ effectively*, *Phys. Rev.* **D 75** (2007) 034016 [hep-ph/0612156].

[15] F. Krüger, *Angular distribution in $B \to K^*(\to K\pi)\ell^+\ell^-$*, in *The discovery potential of a super B factory*, J. Hewett et al., section 2.17 pg. 77, Proceedings of *SLAC Workshops*, Stanford U.S.A. 2003 [hep-ph/0503261].

[16] C.S. Kim and T. Yoshikawa, *Systematic analysis of $B \to K\pi\ell^+\ell^-$ decay through angular decomposition*, arXiv:0711.3880.

[17] C.-H. Chen and C.Q. Geng, *Analysis of $B \to K^*\ell^+\ell^-$ decays at large recoil*, *Nucl. Phys.* **B 636** (2002) 338 [hep-ph/0203003].

[18] R. Fleischer and I. Dunietz, *CP violation and CKM phases from angular distributions for B_s decays into admixtures of CP eigenstates*, *Phys. Rev.* **D 55** (1997) 259 [hep-ph/9605220].

[19] R. Sinha, *CP violation in B mesons using Dalitz plot asymmetries*, hep-ph/9608314.

[20] B. Grinstein and D. Pirjol, *The forward-backward asymmetry in $B \to K\pi\ell^+\ell^-$ decays*, *Phys. Rev.* **D 73** (2006) 094027 [hep-ph/0505155].

[21] A. Ali, E. Lunghi, C. Greub and G. Hiller, *Improved model-independent analysis of semileptonic and radiative rare B decays*, *Phys. Rev.* **D 66** (2002) 034002 [hep-ph/0112300].

[22] G. Buchalla, G. Hiller and G. Isidori, *Phenomenology of non-standard Z couplings in exclusive semileptonic $b \to s$ transitions*, *Phys. Rev.* **D 63** (2001) 014015 [hep-ph/0006136].

[23] F. Krüger and E. Lunghi, *Looking for novel CP-violating effects in $\bar{B} \to K^*\ell^+\ell^-$*, *Phys. Rev.* **D 63** (2001) 014013 [hep-ph/0008210].

[24] Particle Data Group collaboration, W.M. Yao et al., *Review of particle physics*, *J. Phys.* **G 33** (2006) 1 and 2007 partial update for edition 2008 URL: http://pdg.lbl.gov.

[25] P. Ball and R. Zwicky, *$B_{d,s} \to \rho, \omega, K^*, \phi$ decay form factors from light-cone sum rules revisited*, *Phys. Rev.* **D 71** (2005) 014029 [hep-ph/0412079].

[26] *CKMfitter webpage*, http://ckmfitter.in2p3.fr;
H. Lacker, *CKM matrix fits including constraints on new physics*, arXiv:0708.2731.

[27] CDF collaboration, *A combination of CDF and D0 results on the mass of the top quark*, hep-ex/0703034.

[28] T. Onogi, *Heavy flavor physics from lattice QCD*, PoS(LAT2006)017 [hep-lat/0610115].

[29] V.M. Braun, D.Y. Ivanov and G.P. Korchemsky, *The B-meson distribution amplitude in QCD*, *Phys. Rev.* **D 69** (2004) 034014 [hep-ph/0309330].

[30] P. Ball and R. Zwicky, SU(3) *breaking of leading-twist K and K^* distribution amplitudes: a reprise*, *Phys. Lett.* **B 633** (2006) 289 [hep-ph/0510338].

[31] Belle collaboration, Y. Ushiroda et al., *Time-dependent CP asymmetries in $B^0 \to K^0_S \pi^0 \gamma$ transitions*, *Phys. Rev.* **D 74** (2006) 111104 [hep-ex/0608017];
BABAR collaboration, B. Aubert et al., *Measurement of the time-dependent CP asymmetry in $B^0 \to K^{*0}\gamma$ decays*, arXiv:0708.1614.

JHEP07(2008)106

[32] CDF collaboration, T. Aaltonen et al., *Search for $B_s \to \mu^+\mu^-$ and $B_d \to \mu^+\mu^-$ decays with $2\,fb^{-1}$ of $p\bar{p}$ collisions*, *Phys. Rev. Lett.* **100** (2008) 101802 [arXiv:0712.1708].

[33] BABAR collaboration, B. Aubert et al., *Measurement of the $B \to X_s\ell^+\ell^-$ branching fraction with a sum over exclusive modes*, *Phys. Rev. Lett.* **93** (2004) 081802 [hep-ex/0404006];
BELLE collaboration, K. Abe et al., *Improved measurement of the electroweak penguin process $B \to X_s\ell^+\ell^-$*, hep-ex/0408119;
BELLE collaboration, M. Iwasaki et al., *Improved measurement of the electroweak penguin process $B \to X_s\ell^+\ell^-$*, *Phys. Rev.* **D 72** (2005) 092005 [hep-ex/0503044].

[34] M. Misiak et al., *The first estimate of $B(\bar{B} \to X_s\gamma)$ at $O(\alpha_s^2)$*, *Phys. Rev. Lett.* **98** (2007) 022002 [hep-ph/0609232];
M. Misiak and M. Steinhauser, *NNLO QCD corrections to the $\bar{B} \to X_s\gamma$ matrix elements using interpolation in m_c*, *Nucl. Phys.* **B 764** (2007) 62 [hep-ph/0609241].

[35] T. Huber, E. Lunghi, M. Misiak and D. Wyler, *Electromagnetic logarithms in $\bar{B} \to X_s\ell^+\ell^-$*, *Nucl. Phys.* **B 740** (2006) 105 [hep-ph/0512066].

[36] T. Hurth, E. Lunghi and W. Porod, *Untagged $B \to X_{s+d}\gamma$ CP asymmetry as a probe for new physics*, *Nucl. Phys.* **B 704** (2005) 56 [hep-ph/0312260].

[37] D. Atwood, M. Gronau and A. Soni, *Mixing-induced CP asymmetries in radiative B decays in and beyond the standard model*, *Phys. Rev. Lett.* **79** (1997) 185 [hep-ph/9704272].

[38] D. Guetta and E. Nardi, *Searching for new physics in rare $B \to \tau$ decays*, *Phys. Rev.* **D 58** (1998) 012001 [hep-ph/9707371];
S. Fukae, C.S. Kim, T. Morozumi and T. Yoshikawa, *A model independent analysis of the rare B decay $B \to X_s\ell^+\ell^-$*, *Phys. Rev.* **D 59** (1999) 074013 [hep-ph/9807254].

[39] B. Grinstein and D. Pirjol, *Precise $|V_{ub}|$ determination from exclusive B decays: controlling the long-distance effects*, *Phys. Rev.* **D 70** (2004) 114005 [hep-ph/0404250].

[40] B. Grinstein, Y. Grossman, Z. Ligeti and D. Pirjol, *The photon polarization in $B \to X\gamma$ in the standard model*, *Phys. Rev.* **D 71** (2005) 011504 [hep-ph/0412019].

[41] P. Ball, G.W. Jones and R. Zwicky, *$B \to V\gamma$ beyond QCD factorisation*, *Phys. Rev.* **D 75** (2007) 054004 [hep-ph/0612081].

[42] C. Bobeth, G. Hiller and G. Piranishvili, *Angular distributions of $B \to K\bar{\ell}\ell$ decays*, *JHEP* **12** (2007) 040 [arXiv:0709.4174].

[43] J.H. Lopez, *Sensitivity studies of the decay $B_d^0 \to K^{*0}(K^+\pi)\mu^+\mu^-$ at LHCb*, public preprint LHCb-2005-010.

[44] C. Bobeth, M. Misiak and J. Urban, *Photonic penguins at two loops and m_t-dependence of $BR(B \to X_s\ell^+\ell^-)$*, *Nucl. Phys.* **B 574** (2000) 291 [hep-ph/9910220].

[45] K.G. Chetyrkin, M. Misiak and M. Münz, *Weak radiative B-meson decay beyond leading logarithms*, *Phys. Lett.* **B 400** (1997) 206 [*Erratum ibid.* **B 425** (1998) 414] [hep-ph/9612313].

[46] A.J. Buras, M. Misiak, M. Münz and S. Pokorski, *Theoretical uncertainties and phenomenological aspects of $B \to X_s\gamma$ decay*, *Nucl. Phys.* **B 424** (1994) 374 [hep-ph/9311345].

[47] G. Burdman and G. Hiller, *Semileptonic form-factors from $B \to K^*\gamma$ decays in the large energy limit*, *Phys. Rev.* **D 63** (2001) 113008 [hep-ph/0011266].

JHEP07(2008)106

[48] M. Beneke and T. Feldmann, *Symmetry-breaking corrections to heavy-to-light B meson form factors at large recoil*, *Nucl. Phys.* **B 592** (2001) 3 [hep-ph/0008255].